NATIONAL ADVISORY COMMITTEE FOR AERONAUTICS

WARTIME REPORT

ORIGINALLY ISSUED
August 1945 as
Advance Restricted Report L5F25

TESTS OF A LINKED DIFFERENTIAL FLAP SYSTEM DESIGNED TO MINIMIZE THE REDUCTION IN EFFECTIVE DIHEDRAL CAUSED BY POWER

By Marvin Pitkin and Robert O. Schade

Langley Memorial Aeronautical Laboratory
Langley Field, Va.

WASHINGTON

NATIONAL ADVISORY COMMITTEE FOR AERONAUTICS

ADVANCE RESTRICTED REPORT

TESTS OF A LINKED DIFFERENTIAL FLAP SYSTEM DESIGNED TO MINIMIZE THE REDUCTION IN EFFECTIVE DIHEDRAL CAUSED BY POWER

By Marvin Pitkin and Robert O. Schade

SUMMARY

An investigation has been made in the Langley free-flight tunnel to determine experimentally the effects of a linked differential flap system upon the effective-dihedral characteristics of a $\frac{1}{10}$-scale powered airplane model. The differential flap system consisted of two individual flaps so linked as to operate differentially from an initial setting when free and designed to create rolling moments automatically opposing those created by slipstream effects.

Tests were made on the Langley free-flight-tunnel balance and on a trim stand that permitted freedom in roll and yaw.

The results of the tests indicate that the negative dihedral changes caused by power may be materially reduced or completely eliminated by use of a differential flap system. Increasing the flap-differential ratio (ratio of upgoing flap deflection to downgoing flap deflection) to a value above unity increased the effectiveness of the differential flap system in opposing the dihedral changes caused by power but diminished the tendency of the flaps to restore themselves to their initial setting of equal deflection. Little effect was observed when the flap-differential ratio was decreased to a value below unity. Differential flap action also increased the static directional stability.

INTRODUCTION

The application of power in tractor airplanes generally causes a large decrease in the effective dihedral of such airplanes, particularly at low speeds. For airplanes possessing initially small positive values of effective dihedral in gliding flight, power application may lower the effective dihedral to negative values and induce large and unsatisfactory degrees of spiral divergence. These adverse effects cannot be simply eliminated by the expediency of increasing the initial amount of geometric dihedral because such a change may provide an excessive amount of dihedral with power off and lead to poor or unstable oscillatory characteristics in power-off flight or in power-on flight at high speeds.

From the previous considerations, it is desirable to seek means of avoiding large dihedral changes due to power. One possible solution proposed by Dr. H. S. Ribner of the Langley Memorial Aeronautical Laboratory involves use of a system of linkage whereby the flaps operate differentially from an initial setting so as to create rolling moments automatically opposing those created by slipstream effects. The results of tests of such a system in the Langley free-flight tunnel are reported herein.

A powered model, representative of conventional single-radial-engine fighter airplanes, was employed for all tests. Most of the tests were made on a test stand that permitted freedom in roll and yaw. Measurements of rolling moments were obtained by use of a calibrated-spring system. Necessary force-test data were obtained on the Langley free-flight-tunnel six-component balance. The effects of differential flap action upon the dihedral characteristics of the model were studied for various ratios of differential flap movement. In most cases, the tests were made with vertical and horizontal tail surfaces removed, although a brief study was made of the effect of vertical-tail area upon the effective dihedral.

SYMBOLS

The coefficients and symbols are defined as follows:

C_L	lift coefficient (L/qS)
C_D	drag coefficient (D/qS)
C_X	longitudinal-force coefficient (X/qS)
C_l	rolling-moment coefficient (L/qbS)
C_{l_β}	rate of change of rolling-moment coefficient with angle of sideslip, per degree $(\partial C_l/\partial \beta)$
C_{l_ψ}	rate of change of rolling-moment coefficient with angle of yaw, per degree $(\partial C_l/\partial \psi)$
L	force along Z-axis, positive when acting upward, pounds; moment about X-axis, positive when it tends to depress right wing, foot-pounds
X	force along X-axis, positive when acting forward, pounds
D	force along wind direction, positive when acting rearward, pounds; diameter of propeller, feet
Y	force along Y-axis, positive when acting to the right, pounds
M	moment about Y-axis, positive when it tends to raise nose, foot-pounds
N	moment about Z-axis, positive when it tends to turn nose to right, foot-pounds
q	dynamic pressure, pounds per square foot $\left(\frac{1}{2}\rho V^2\right)$
S	wing area, square feet
c	mean aerodynamic chord, feet
b	wing span, feet
V	airspeed, feet per second

ρ	mass density of air, slugs per cubic foot
α	angle of attack, degrees
ψ	angle of yaw, degrees
β	angle of sideslip, degrees
δ_f	flap deflection, degrees
δ_{f_R}	right-flap deflection, degrees
$d\delta_{f_U}/d\delta_{f_D}$	flap-differential ratio (ratio of upgoing flap deflection to downgoing flap deflection)
$\delta_{f_U}/\delta_{f_D}$	mean flap-differential ratio over the first 20° of incremental up deflection
T_c	thrust disk-loading coefficient (Effective thrust/$\rho V^2 D^2$)
V/nD	propeller advance ratio
n	rotational speed, revolutions per second
ΔC_{L_f}	change in lift coefficient caused by flap deflection
S_t	vertical-tail area, square feet
δ_r	rudder deflection, degrees
δ_{r_L}	left-rudder deflection, degrees

THEORY OF DIFFERENTIAL FLAP ACTION

An important part of the decrease in the effective dihedral parameter C_{l_β} caused by power is produced by the lateral displacement of the slipstream over the trailing wing as the airplane is sideslipped. The lateral center of pressure of the additional lift induced by the slipstream moves outboard from its original center position and creates a rolling moment about the center of gravity of the airplane. The

variation of this rolling moment with sideslip angle is such as to reduce the effective dihedral.

On a wing with a flap, the increase in lift of the trailing wing caused by slipstream displacement is accompanied by an increase in flap hinge moment. The hinge moment of the flap mounted on the leading wing similarly is decreased when the airplane is sideslipped.

The flap system tested is shown in figure 1 and is so designed as to utilize the change of flap hinge moments caused by power in order that the dihedral changes caused by power may be reduced. The system consists of two flaps connected by a mechanical linkage. The arrangement of the control rods and singletree is such that upward deflection of one flap pivots the singletree about its fixed center pivot and thus causes downward deflection of the flap on the opposite wing. The central bar, which provides the fulcrum for the differential action, is used to deflect or retract both flaps equally and is extended and locked in flap-down flight.

When the applied hinge moment on the differential flaps changes because of slipstream displacement, the trailing-wing flap tends to rise and the leading-wing flap tends to fall. As the trailing-wing flap rises, its aerodynamic hinge moments decrease whereas those of the leading-wing flap increase. At some differential setting, equilibrium is again obtained. The aileron effect of the differential-flap deflections produces rolling moments that tend to compensate the rolling moments created by slipstream displacement. In addition to direct slipstream-displacement effects, augmentation by the slipstream of the wing-fuselage interference may make an important contribution to the loss in effective dihedral due to power for low-wing airplanes. The effect, however, of such a contribution upon the flap hinge moments would probably be similar to that due to the direct effects of slipstream displacement and, consequently, the basic theory would not be greatly altered.

The preceding considerations indicate that differential flaps are fundamentally a linked-aileron system drooped to some initial downward setting and having an upfloating tendency. Aileron-linkage theory (reference 1) shows that the operating moments of such

a system can be reduced if the ailerons, starting from equal deflections, are so linked that the upgoing aileron deflects at a progressively greater rate than the downgoing aileron (that is, when the values of the flap-differential ratio $d\delta_{f_U}/d\delta_{f_D}$ are greater than unity). The effectiveness of a differential flap system in producing rolling moments opposing those created by power can therefore be increased by increasing the differential ratio of the system above unity, because such a change reduces the restoring moments of the system and thus results in greater incremental flap deflections for a given hinge-moment change induced by power effects. At some differential ratio, the flap system is neutrally balanced and has no tendency to return to the original condition of equilibrium. Differential ratios greater than this value create an overbalanced flap system.

APPARATUS

Wind Tunnel

The tests were conducted in the Langley free-flight tunnel; a complete description of the tunnel is given in reference 2. The free-flight-tunnel six-component balance used in the force tests is described in reference 3. Figure 2 shows the test model mounted on the balance strut in a yawed attitude. All force and moment measurements obtained from this balance are with respect to stability axes. The stability axes (see fig. 3) are a system of axes having their origin at the center of gravity of the airplane and in which the Z-axis is in the plane of symmetry of the airplane and is perpendicular to the relative wind, the X-axis is in the plane of symmetry and perpendicular to the Z-axis, and the Y-axis is perpendicular to the plane of symmetry.

Trim Stand

Most of the tests were made on a trim stand that was so constructed as to allow the model freedom in roll and yaw about the stability axes. The construction of the stand is illustrated in the sketch shown as figure 4.

A photograph of the model mounted on the trim stand is shown in figure 5. As shown in figure 4, a calibrated spring was attached to the roll-free bearing for the tests to provide for stability in roll and to permit unbalanced rolling moments to be obtained as a function of the angle of bank. The angle of bank was read visually by means of the calibrated indicator card shown in figure 5. Flap deflections were also read directly from an indicator card by means of a pointer rigidly attached to the inboard end of the left-flap segment. (See fig. 5.)

Model

The model used in the investigation is generally representative of low-wing radial-engine fighter airplanes and corresponds to a $\frac{1}{10}$-scale model of a 40-foot-span airplane. A three-view drawing of the model is shown as figure 6 and photographs of the model are shown in figure 7. The dimensional characteristics of the full-scale airplane as represented by the $\frac{1}{10}$-scale model tested in the Langley free-flight tunnel are as follows:

Propeller:	
Diameter, feet	11.7
Number of blades	2
Wing:	
Area, square feet	266.5
Span, feet	40
Aspect ratio	5.71
Airfoil section	Rhode St. Genese 35
Incidence at root, degrees	0
Dihedral, degrees	0
Sweepback at quarter percent chord line, degrees	3.2
Taper ratio	2:1
Mean aerodynamic chord, inches	83.90
Root chord, inches	107.80
Center of gravity:	
Back of leading edge of root chord, inches	32.91
Below fuselage center line, inches	0
Percent of mean aerodynamic chord	25

Flaps:

Type	Split, partial span
Span, feet	20
Percent wing span	50

Tail:

Vertical tail 1	
Total area, square feet	13.34
Percent wing area	5
Vertical tail 2	
Total area, square feet	26.68
Percent wing area	10
Vertical tail 3	
Total area, square feet	40.0
Percent wing area	15

The model was equipped with a 14.0-inch diameter, two-blade propeller set at an angle of pitch of 10° at 0.75 radius and was powered by a direct-current controllable-speed electric motor rated $1\frac{1}{2}$ horsepower at 12,000 rpm. The propeller was attached to the motor by direct drive, and an electrical tachometer was installed on the motor to permit direct measurements of propeller speed. Right-hand propeller rotation was used for all tests. The layout of the isolated power unit mounted on the roll bracket is shown in figure 8.

The model was equipped with partial-span split flaps of 25 percent chord and of total span 50 percent of the wing span. The flaps when locked and not in differential operation were at an initial setting of 40°. The right- and left-wing flaps were linked together through a differential linkage located in the fuselage. Details of the flap linkage are shown in the photograph presented in figure 9. This linkage system was designed to permit variation of the flap-differential ratio (ratio of upgoing flap deflection to downgoing flap deflection). This result was accomplished by moving the two end pivots of the singletree rearward with respect to the fixed central pivot. The linkage system was so arranged as to permit maximum differential flap deflections of 37.5° down and 25° up from the initial flap setting of 40° down.

The Rhode St. Genese 35 airfoil section was used on the model wing because of the high maximum lift coefficient of this section at the low Reynolds numbers at which the tests were run. The geometric dihedral of the model measured from the lower surface was set at 0° for all tests.

No horizontal tail surfaces were used on the model. Three similar vertical tail surfaces of different areas were installed on the model for some tests. Sketches of these tail surfaces are shown in figure 10.

TESTS

Test Conditions

All tests were run at a dynamic pressure of 1.90 pounds per square foot, which corresponds to an airspeed of about 27 miles per hour at standard sea-level conditions and to a test Reynolds number of 172,000 based on the mean aerodynamic chord of 0.67 foot. All forces and moments measured in the tests are with respect to the stability axes (fig. 3), which intersect at a point located at 25 percent mean aerodynamic chord and on the center line (thrust line) of the fuselage. In order to obtain sizeable power effects upon the effective dihedral all power-on tests were made at $T_c = 0.96$, a value that represented the maximum thrust obtainable from the motor-propeller unit. This value simulated full-scale brake horsepowers ranging from approximately 3000 to 9000 over the high-lift range.

Force Tests

Force tests were made with power on and with propeller off, and with flaps undeflected and deflected 40° for various angles of attack and yaw. Some tests were made with power on at angles of attack of 1.0° and 13.5° and at yaw angles of 0° and ±10° to determine the effectiveness of the flap system. For these tests the flap on the left wing was locked at 0° and the deflection of the flap on the right wing was varied from 0° to 70°.

A complete thrust calibration of the propeller-motor unit was made to determine the model power characteristics.

A plot of the results of this calibration is presented as figure 11.

Trim-Stand Tests

Trim-stand tests were made to determine the effect of freeing the differential flaps on the effective dihedral of the test model. The influence of flap-differential ratio upon the effective-dihedral characteristics was also studied. Other tests were made to determine the effect of vertical-tail area upon the effective dihedral and the influence of differential flap action upon the directional stability.

Test procedure.- The effective-dihedral characteristics of the model with tail surfaces removed were determined as follows:

The model was set at various angles of yaw on the test stand and the corresponding trim angles of bank for the propeller-off and power-on conditions were noted by visual observation. The values of the angles of bank thus obtained were converted to rolling-moment coefficients by means of the roll-spring calibration. The effective-dihedral parameter C_{l_β} (or $-C_{l_\psi}$) was then directly determined from a plot of these rolling-moment coefficients against the corresponding angles of yaw. The same procedure for determining the effective-dihedral characteristics of the model with vertical tail surfaces installed was followed except that the model was free in yaw and was trimmed at the different angles of yaw by rudder deflection.

Calibration curves were obtained for each flap linkage by measuring the upgoing flap deflection produced by a given downgoing deflection on the opposite wing. Representative calibration curves obtained in this manner are shown in figure 12. It should be noted that these curves are nonlinear. This nonlinearity is characteristic of the linkage system employed and results in a change of flap-differential ratio $d\delta f_U/d\delta f_D$ with incremental flap deflection. For definiteness, the term "flap-differential ratio" was defined by the mean slope of the differential curves over the first 20° of incremental up deflection. This procedure is considered

sufficient to identify the general effects of altering flap-differential ratio in the tests.

Scope of trim-stand tests.- Trim-stand tests were made to determine the dihedral characteristics of the model for the following conditions:

(1) Flaps locked at 40°; propeller off; $\alpha = 1.0°$; $C_L = 0.93$

(2) Flaps locked at 40°; $T_c = 0.96$; $\alpha = 1.0°$ and 13.5°; $C_L = 1.4$ and 2.7

(3) Flaps free; $T_c = 0.96$; $\alpha = 1.0°$ and 13.5°; $C_L = 1.4$ and 2.7

Propeller-off tests were not run at 13.5° angle of attack because the model was completely stalled at that angle. The effect of varying the flap-differential ratio between 0.8 and 1.4 was studied for condition (3). The effect of vertical-tail area upon the power-on ($T_c = 0.96$) dihedral characteristics was investigated at an angle of attack of 13.5° with flaps locked and with flaps free at a differential ratio of 1.0.

RESULTS AND DISCUSSION

The results of the tests are given in figures 13 to 25. Lift and drag data obtained from the force tests are given in figures 13 to 15 for various power and flap configurations. These data show that maximum lift coefficients comparable with those obtained on full-scale airplanes were obtained for all test conditions.

Effective-Dihedral Characteristics

Effect of power.- The effect of power application upon the effective-dihedral characteristics of the model with flaps locked at 40° is shown in figure 16. These data show that application of power increased the negative slope of the curve of rolling-moment against yaw angle from -0.00063 to -0.00205. This change corresponds to reduction of about 7° in effective dihedral and illustrates the usual effect of power upon the dihedral parameter.

Because of the particular geometric configuration used in the tests, the test model possessed 2° negative effective dihedral in the propeller-off condition. The model differed therefore from conventional full-scale airplanes, which generally possess moderately large positive effective dihedral in the propeller-off condition. This difference, however, is only of academic interest inasmuch as the reduction in effective dihedral caused by power is an incremental effect that is considered independent of the initial value of dihedral in the propeller-off condition.

The data of figure 16 also indicate little effect of lift coefficient upon the dihedral characteristics of the model under conditions of constant thrust coefficient. This phenomenon is unusual inasmuch as an increase in lift coefficient generally results in an increase in power effects. The increase in effective dihedral generally associated with increasing angle of attack (lift coefficient) was probably sufficient at high angles of attack to offset the increased power effects caused by the same increase in angle of attack.

The action of the slipstream in producing dihedral changes, previously discussed in the section "Theory of Differential Flap Action," appears to be verified by the results of force tests made to determine the flap effectiveness with power on (figs. 17 and 18). These data show that when the model was yawed to the right ($\psi = 10°$) the lift increments contributed by the flap on the right (trailing) wing were considerably increased because of the action of the displaced slipstream. The reverse was true when the model was yawed to the left ($\psi = -10°$).

Effects of differential flap action.- Trim-stand-test data showing the effect of freeing the differential flaps on the effective dihedral are given in figure 19. Figure 19(a) shows little effect with propeller off; whereas figure 19(b) shows that with power on for a differential ratio of 1.0 (equal up and down flap deflections), the negative dihedral change caused by power at a lift coefficient of 1.4 was reduced by over 80 percent. A similar effect of differential flap action was also attained at a lift coefficient of 2.7.

Additional data showing the effect of varying flap-differential ratio are shown in figure 20. The slopes of these curves, which are indicative of the

effective-dihedral characteristics, are shown plotted against mean flap-differential ratio in figure 21. The results presented in figure 21 indicate that, although decreasing the differential ratio below unity slightly reduced the efficacy of the differential flaps in opposing dihedral changes due to power, increasing the flap-differential ratio above unity was benificial. The data show that the adverse effects of power upon the effective dihedral were completely eliminated when a differential ratio of about 1.04 was used at a lift coefficient of 1.4 or when a differential ratio of about 0.96 was used at a lift coefficient of 2.7. Use of ratios greater than these values reversed the effect of power and resulted in positive increases in the effective-dihedral parameter with power application. Slightly larger effects of differential ratio were usually encountered at the high-lift condition (C_L = 2.7). These differential-ratio tests showed that the differential flap system employed in the tests became overbalanced at differential ratios of about 1.4. When overbalance occurred, the flaps locked violently against their stops as soon as power was applied, thereby inducing large and abrupt rolling motions. This action occurred for all angles of yaw.

The beneficial effect of increasing flap-differential ratio is in agreement with the theory of reference 1. As shown by the data in figure 22, increasing flap-differential ratio generally resulted in greater incremental flap deflections at a given angle of yaw as a result of reduced unbalance of the flap system.

Effect of vertical-tail area.- Results of tests made to determine the influence of vertical-tail area upon the power-on effective-dihedral characteristics of the model are presented in figure 23 and are summarized in figure 24. These data show that adding vertical-tail area up to 15 percent of the wing area had little effect. The general tendency of such additions, however, was to increase the effective dihedral.

Directional Stability Characteristics

Rudder-deflection data from the yaw-free tests (fig. 25) indicate that differential flap action considerably increased the static directional stability. This increase in stability is attributed to the drag

changes accompanying the differential action. As the airplane is yawed, the flap on the trailing wing moves up and reduces the drag of that wing, whereas the flap on the leading wing moves down and increases the drag. These drag changes produce stabilizing yawing moments. Although no yaw-free tests were made at differential ratios other than 1.0, it appears reasonable to assume that increasing the differential ratio will increase the stabilizing action of the flaps in yaw because the larger flap deflections encountered will cause greater drag increments.

Remarks about Design

Dynamic response.- In brief tests made to determine the dynamic response of the flap system to sudden and sharp yawing motions, the results (obtained by visual observation) indicated no appreciable lag of flap deflection with yawing motion. It should be emphasized, however, that the friction in the flap system in the current tests was held to small values, perhaps smaller than those encountered in full-scale designs. Inasmuch as excessive friction in the flap system could cause the controls to "freeze" in a differential attitude (particularly for small degrees of balance) and thus to induce violent rolling maneuvers, the designer should attempt to limit the friction in the flap system to as small a value as is practical.

Linkage design.- The principle of the differential flap linkage is not necessarily restricted to the mechanical, pin-jointed type of system. Although differential ratios other than unity are readily obtained with this type of system, differential flaps could also be linked by means of hydraulic, cam, gearing, or electrical systems.

Aerodynamic balance.- Because of the severity of the rolling motions caused by an overbalanced flap system, care should be taken in the design of differential flap systems to allow a safe margin of unbalance. Further analytical and experimental work with particular reference to the effects of nonlinearity of flap load and moment characteristics is required to establish a quantitative design procedure for differential flap systems.

CONCLUSIONS

The following conclusions have been drawn from tests of a differential flap system installed in a $\frac{1}{10}$-scale powered airplane model in the Langley free-flight tunnel:

1. A flap system in which the right and left flaps were linked together and were free to deflect differentially materially reduced or eliminated negative dihedral changes caused by power application.

2. Increasing the flap-differential ratio of the flap system (ratio of upgoing flap deflection to downgoing flap deflection) above unity increased the effectiveness of the flap system in opposing dihedral changes caused by power.

3. Increasing the flap-differential ratio of the flap system reduced and eventually reversed the aerodynamic tendency of the flaps to restore themselves to their initial setting of equal deflection.

4. Little effect upon the effective-dihedral characteristics was observed when the flap-differential ratio was decreased to a value below unity.

5. Differential flap action caused an increase in the static directional stability of an airplane.

6. Further analytical and experimental study is required to develop a quantitative design procedure for differential flap systems.

Langley Memorial Aeronautical Laboratory
National Advisory Committee for Aeronautics
Langley Field, Va.

REFERENCES

1. Jones, Robert T., and Nerken, Albert I.: The Reduction of Aileron Operating Force by Differential Linkage. NACA TN No. 586, 1936.

2. Shortal, Joseph A., and Osterhout, Clayton J.: Preliminary Stability and Control Tests in the NACA Free-Flight Wind Tunnel and Correlation with Full-Scale Flight Tests. NACA TN No. 810, 1941.

3. Shortal, Joseph A., and Draper, John W.: Free-Flight-Tunnel Investigation of the Effect of the Fuselage Length and the Aspect Ratio and Size of the Vertical Tail on the Lateral Stability and Control. NACA ARR No. 3D17, 1943.

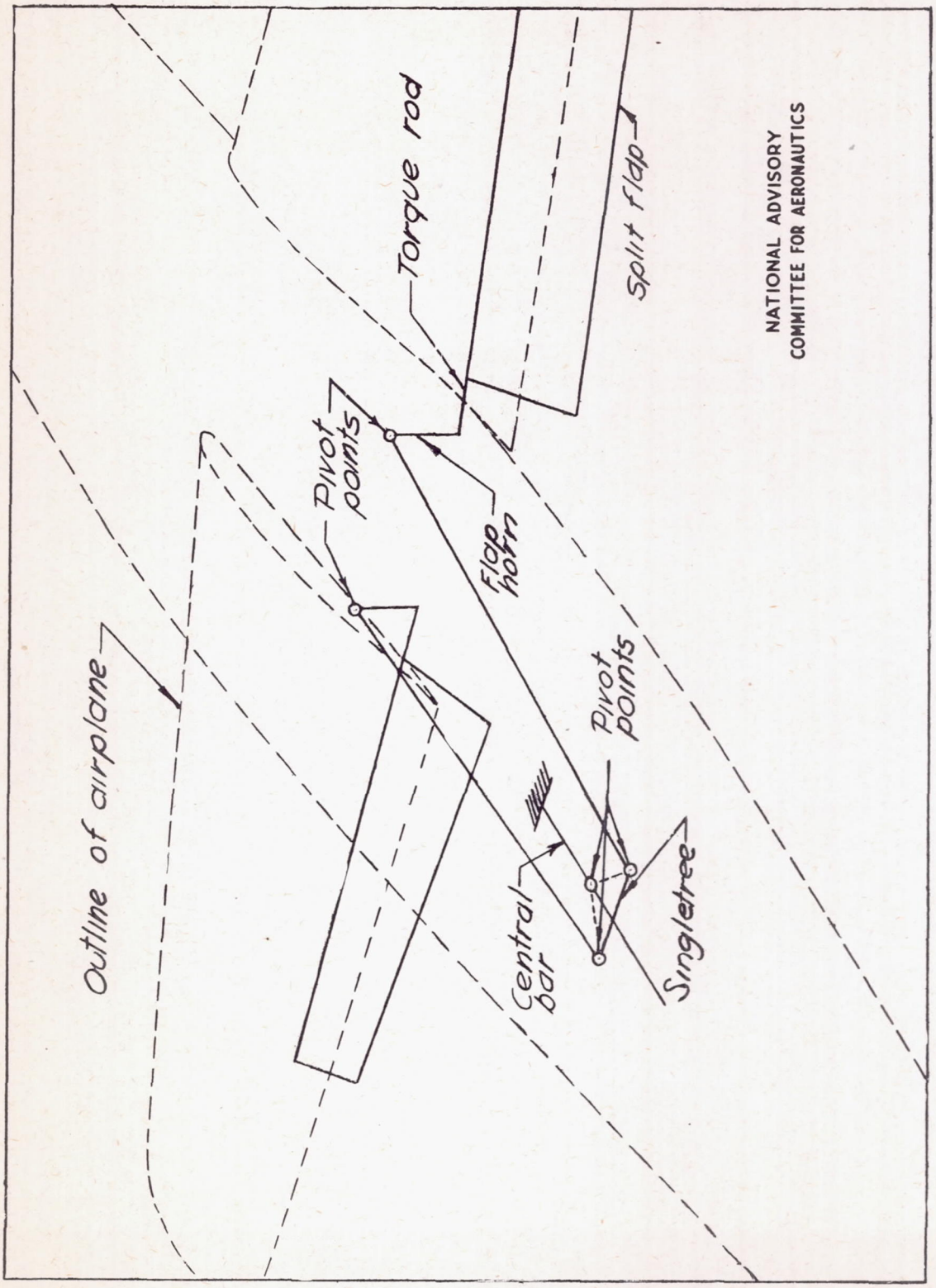

Figure 1.- Sketch of differential flap system.

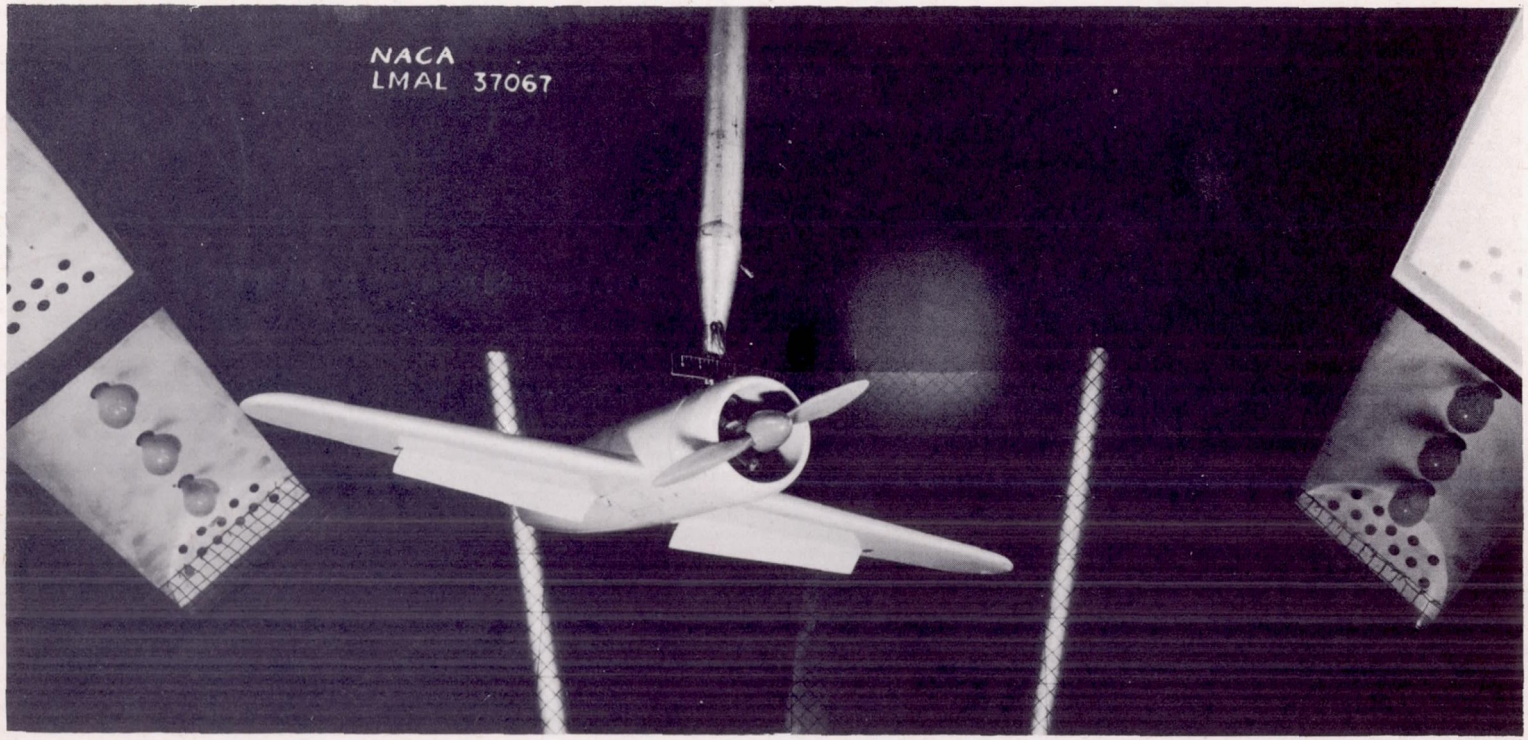

Figure 2.- Photograph of powered test model in yawed attitude mounted on six-component balance in Langley free-flight tunnel.

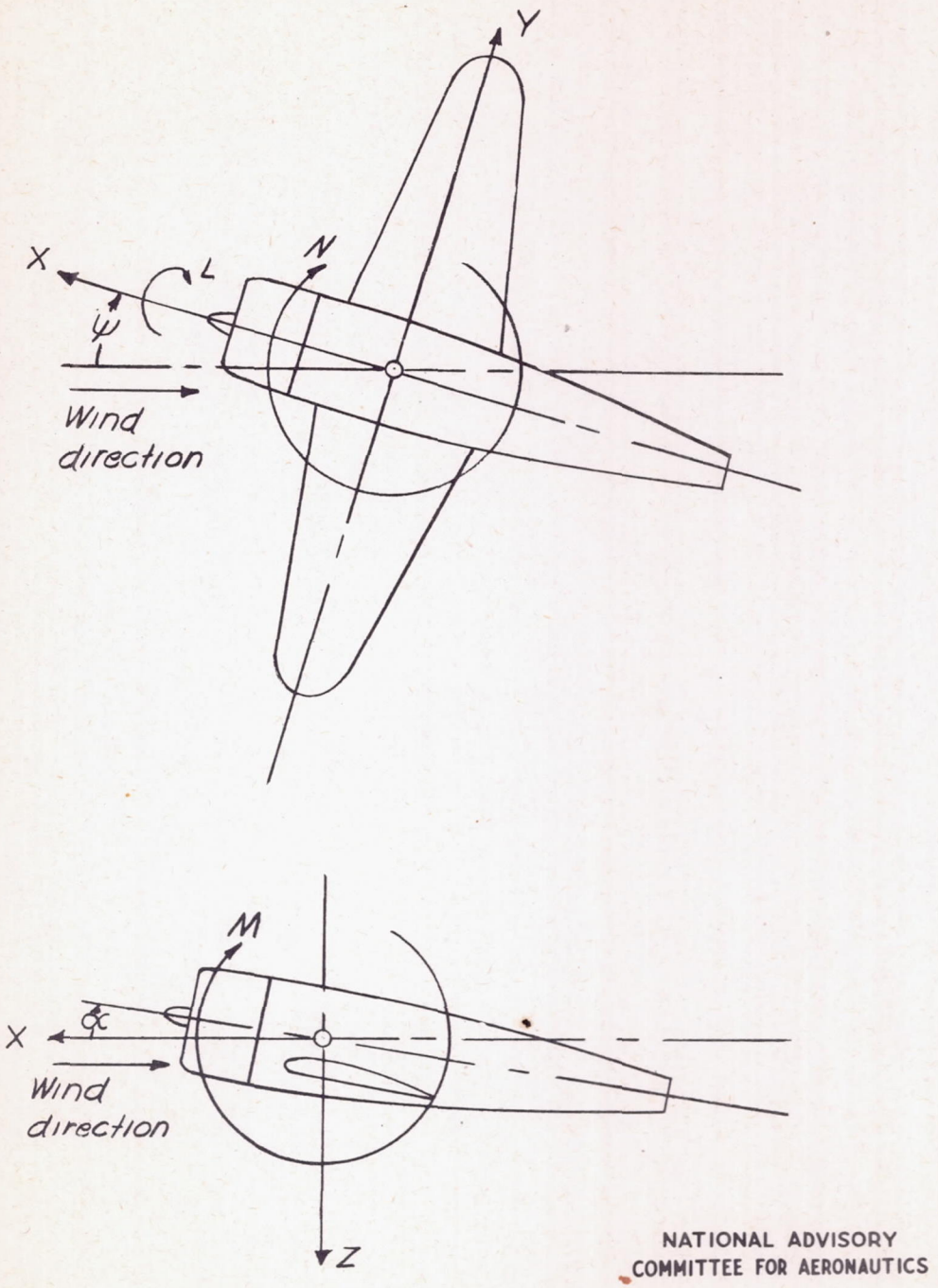

Figure 3.- System of stability axes. Arrows indicate positive directions of moments and forces.

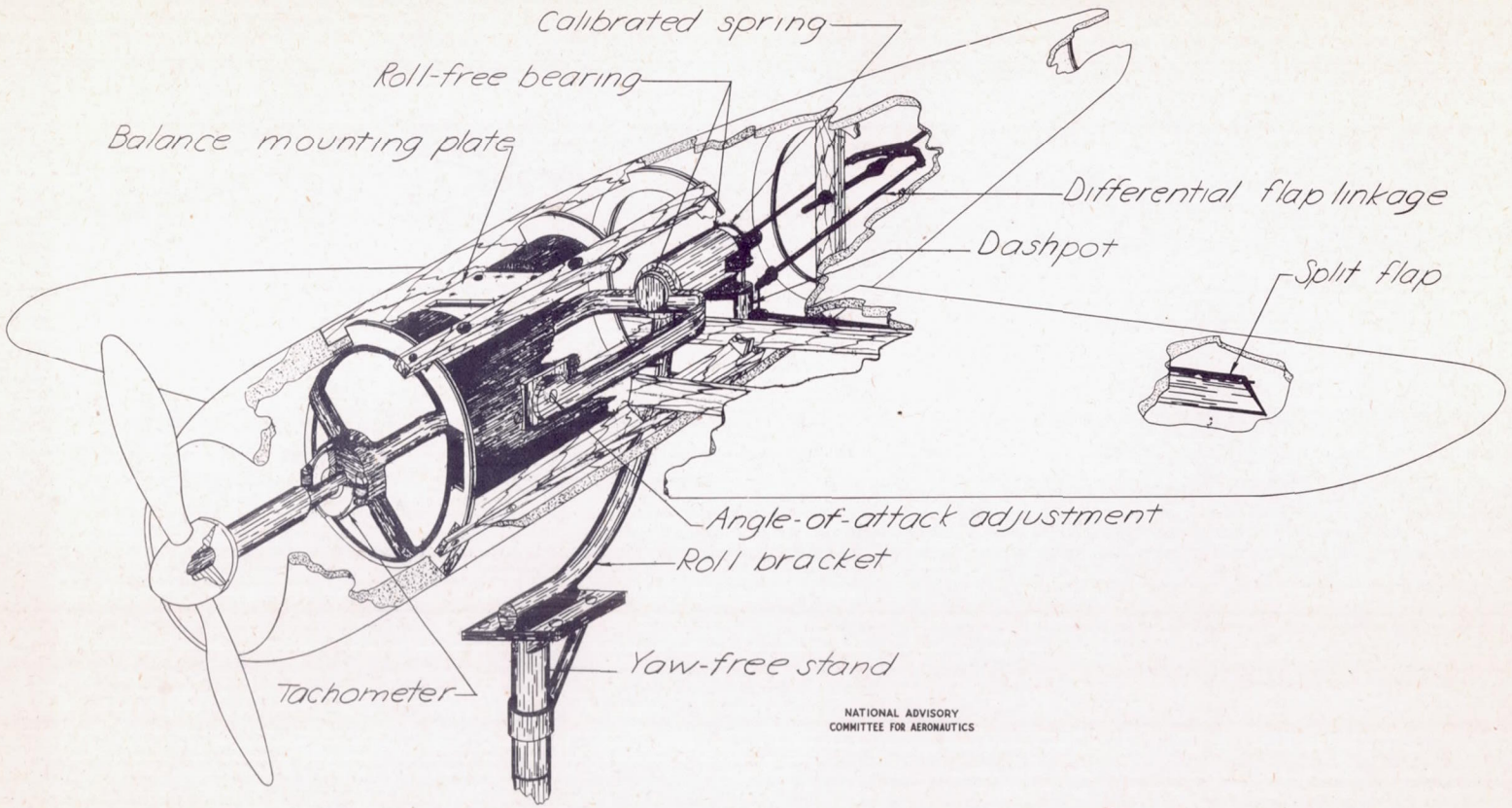

Figure 4.- Sketch of model mounted on trim stand in Langley free-flight tunnel.

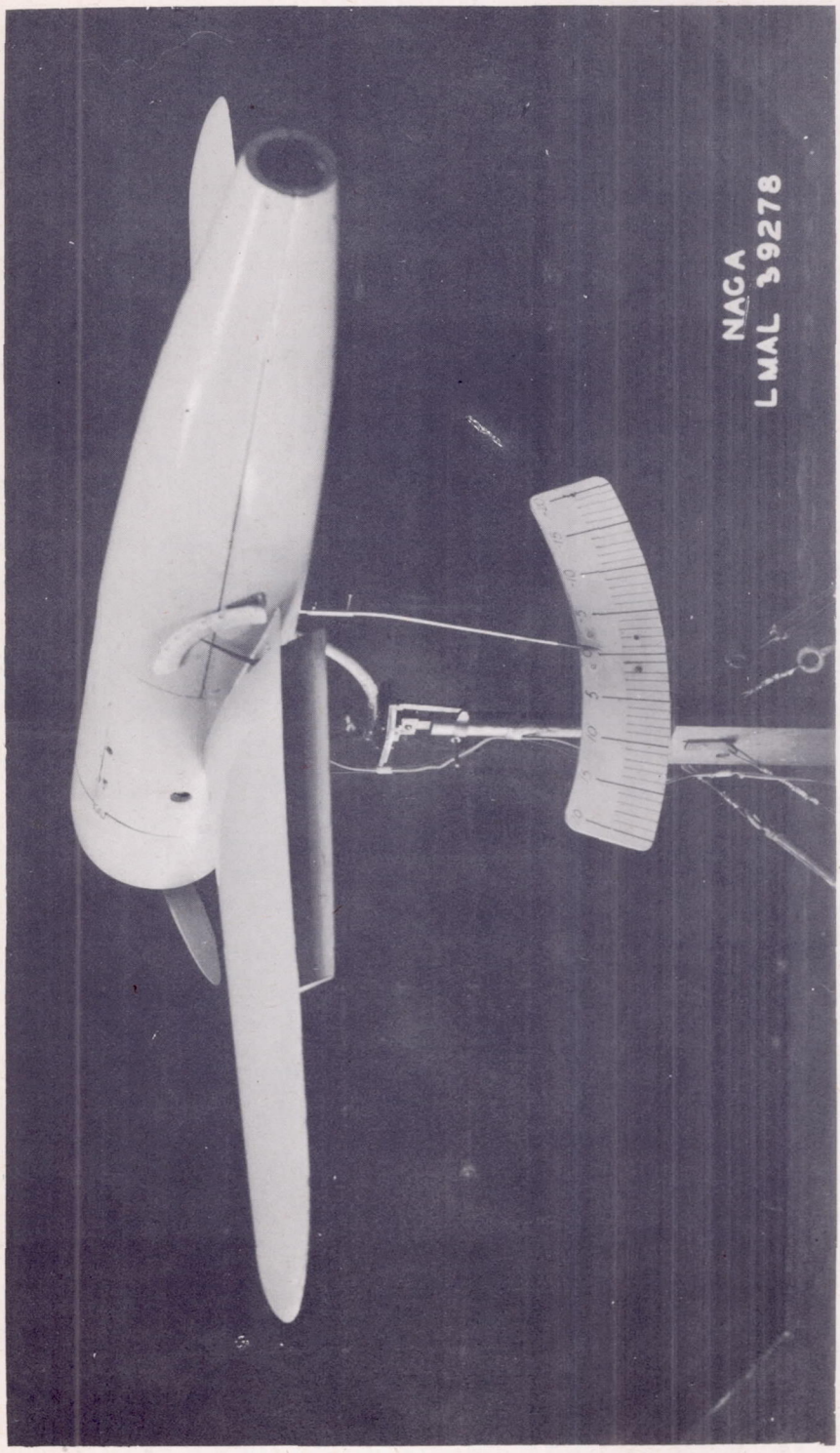

Figure 5.- Photograph of powered test model mounted on trim stand.

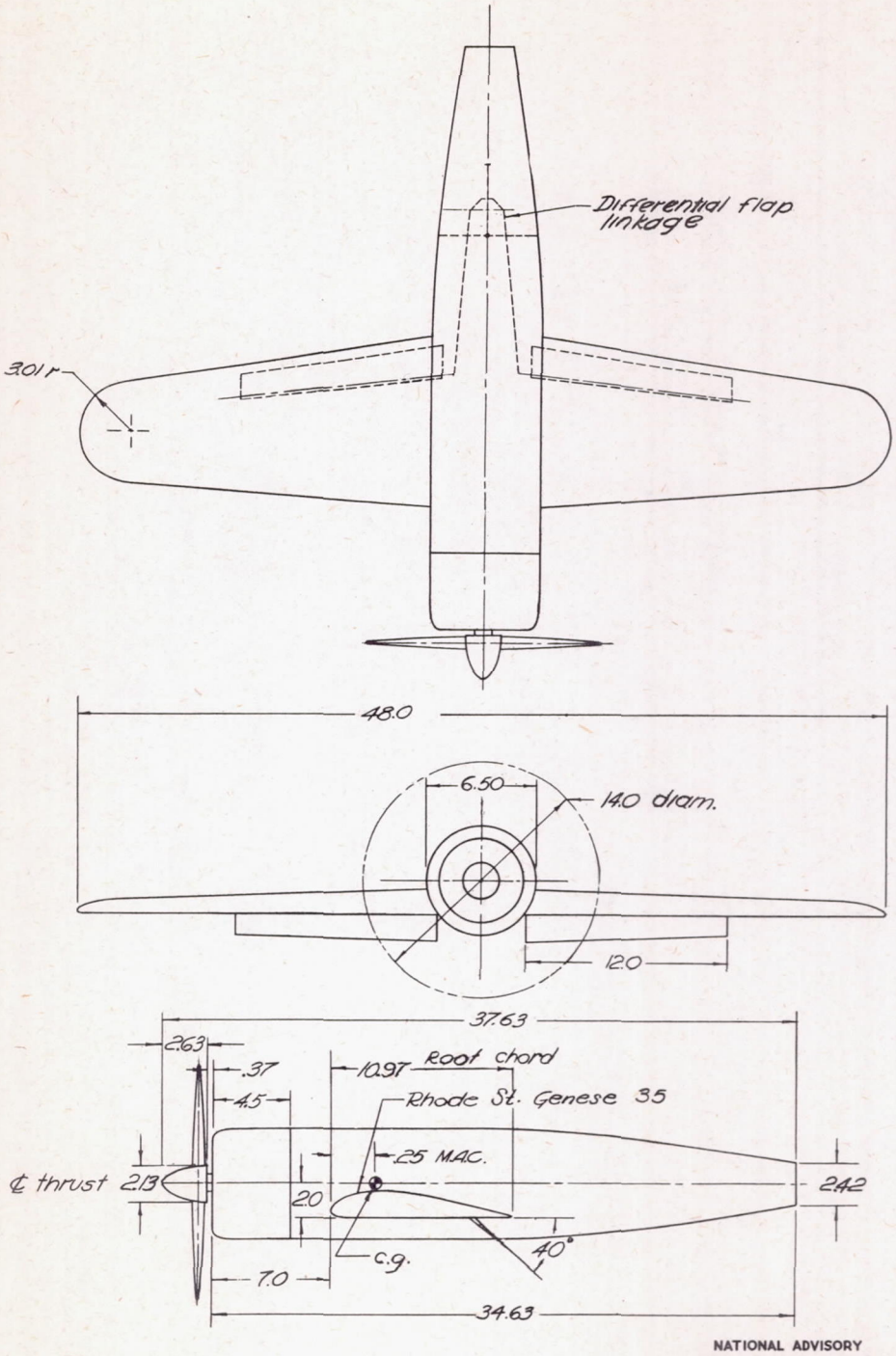

Figure 6.- Three-view sketch of powered test model as tested in Langley free-flight tunnel. Wing incidence = 0°; dihedral angle = 0°; all dimensions in inches.

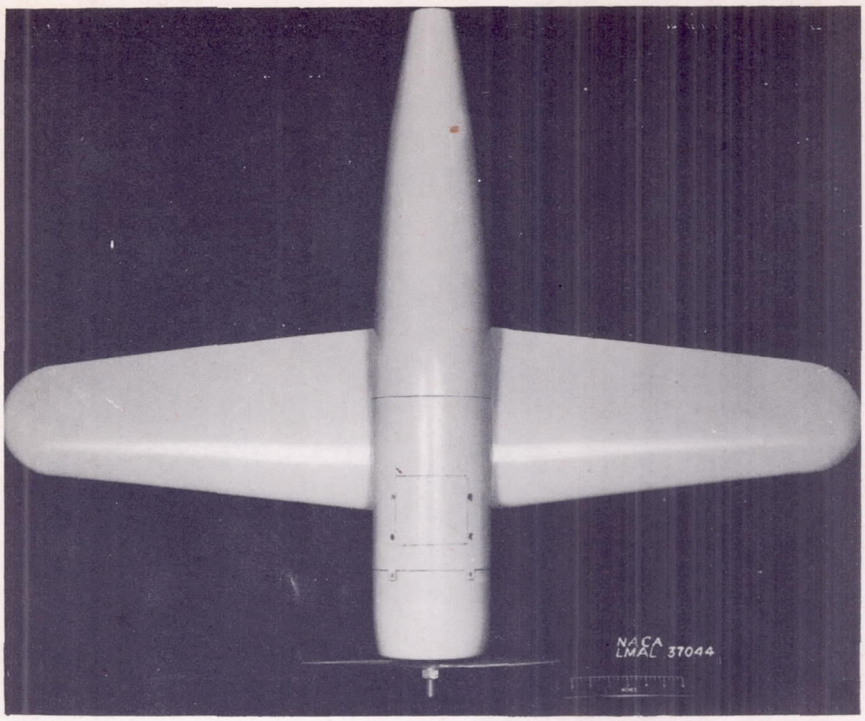

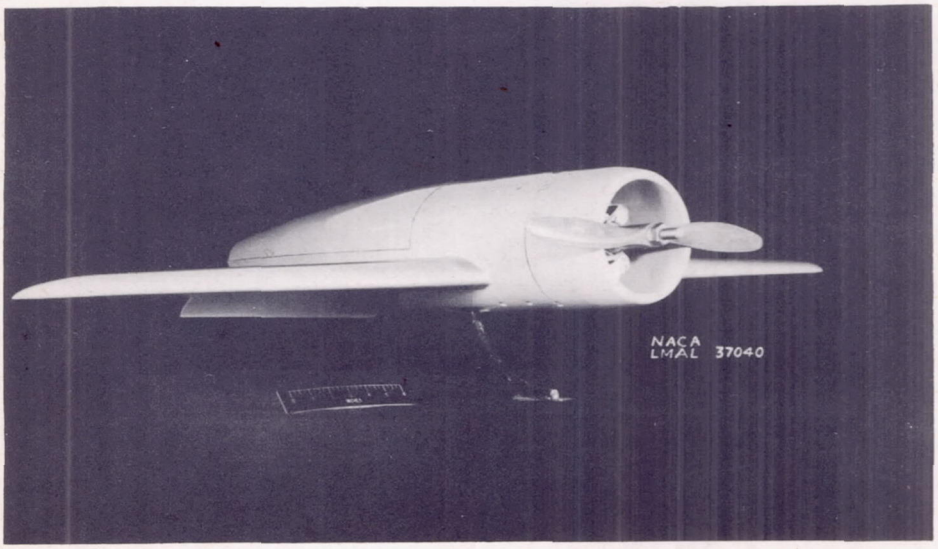

Figure 7.- Photographs of powered model employed in Langley free-flight-tunnel tests.

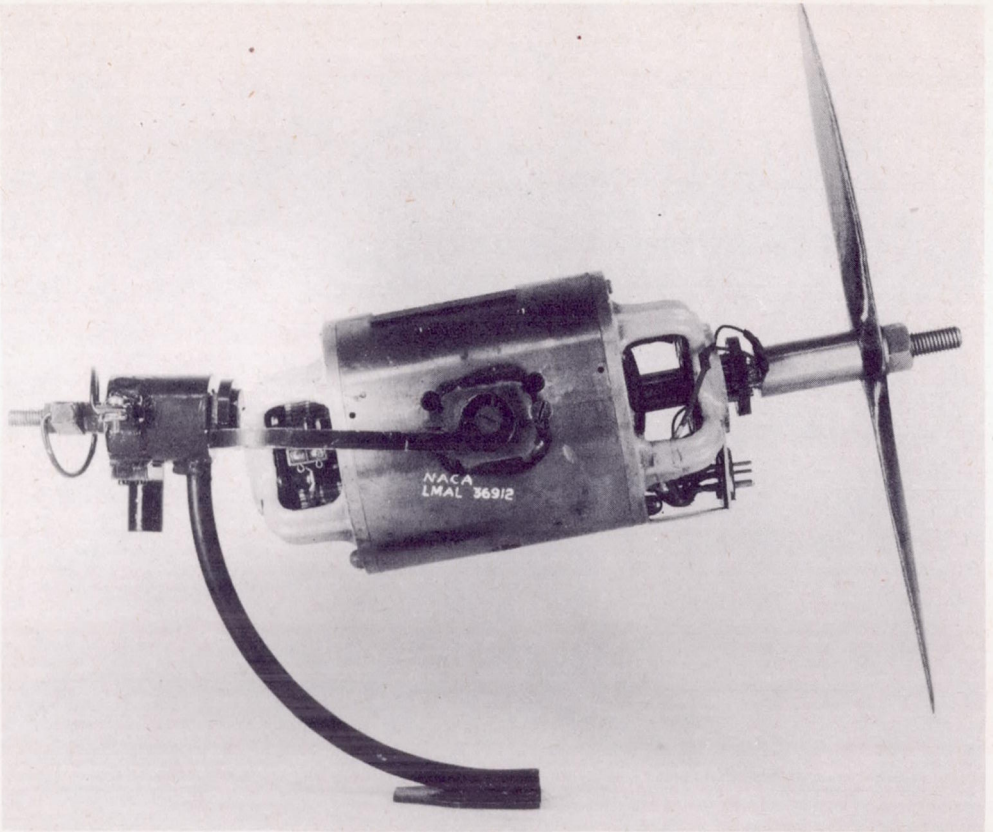

Figure 8.- Photograph of roll bracket and power unit employed in the differential-flap investigation in the Langley free-flight tunnel.

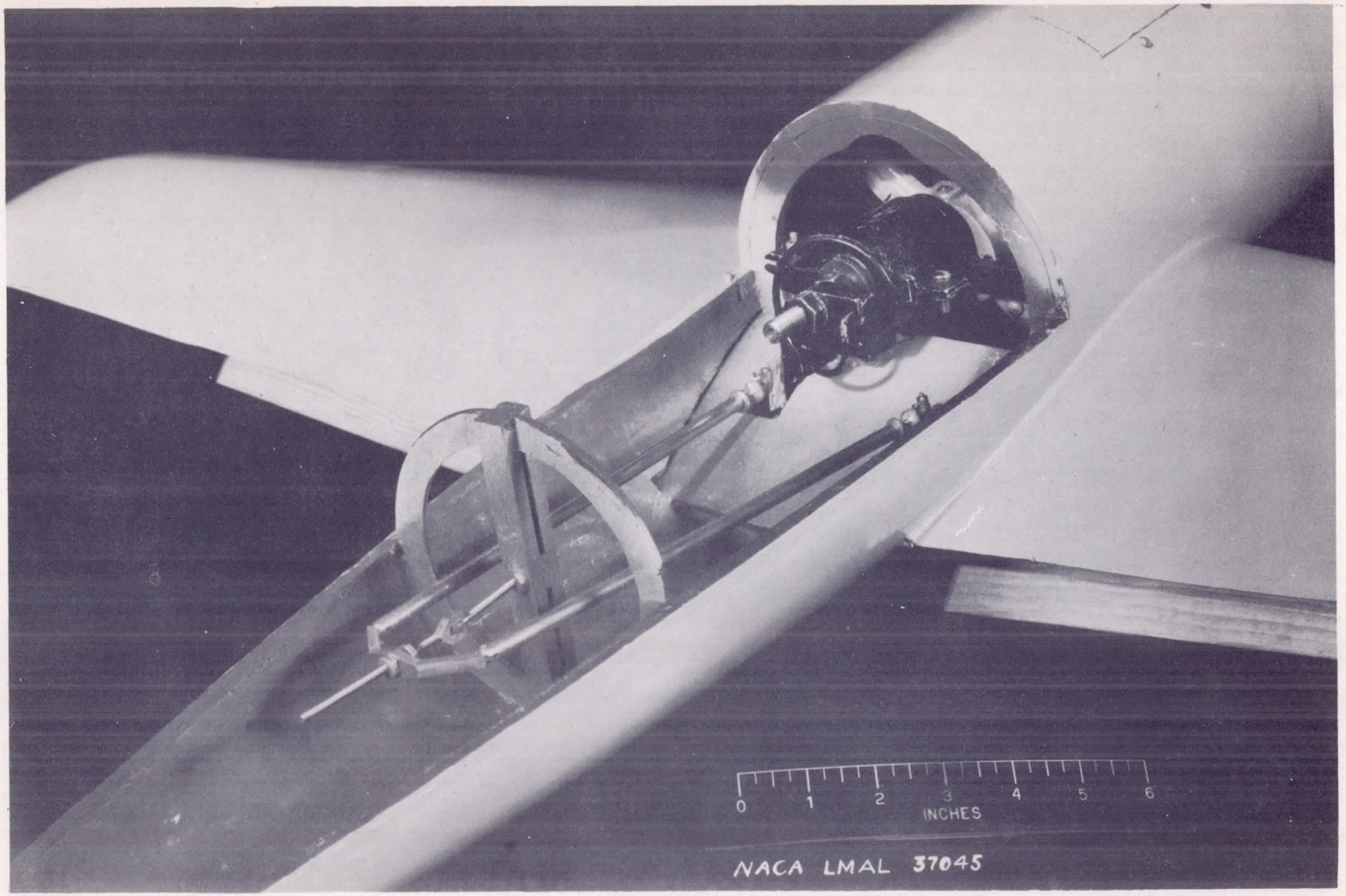

Figure 9.- Photograph of differential flap linkage employed in the Langley free-flight-tunnel tests.

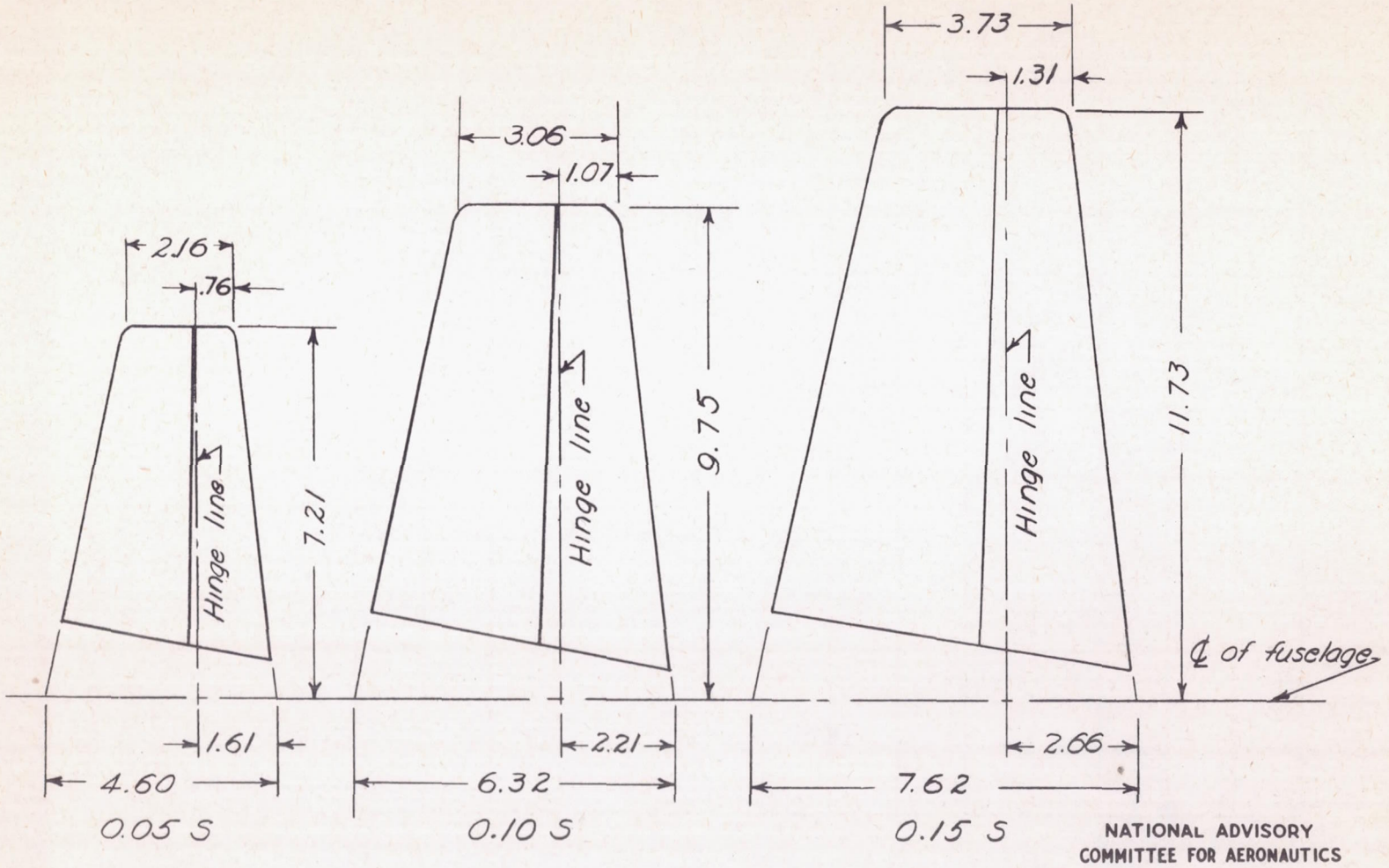

Figure 10.- Sketches of vertical tail surfaces used in Langley free-flight-tunnel tests of a model with differential flaps. Distance from center of gravity to rudder hinge line is 22 inches. All dimensions in inches.

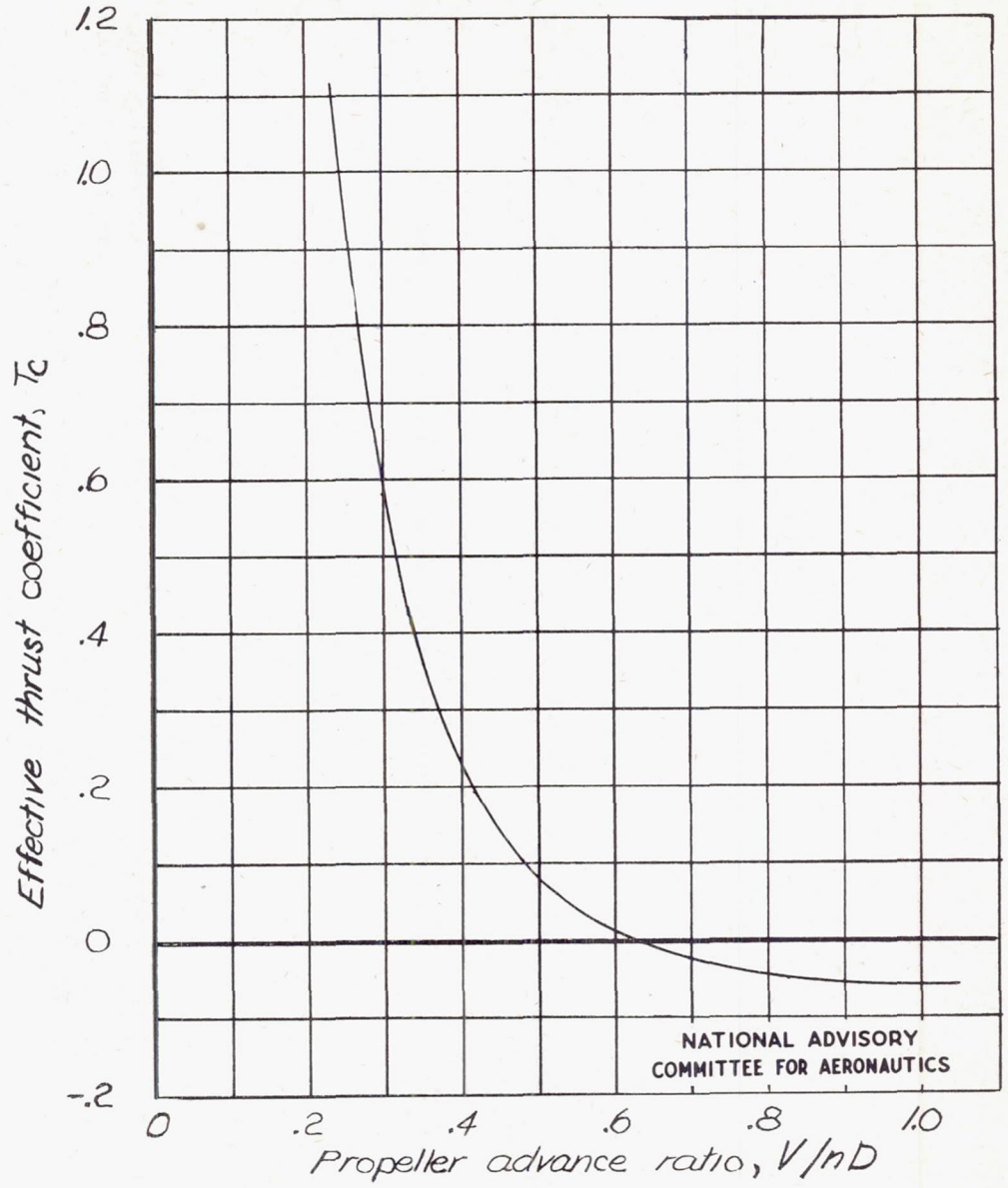

Figure 11.- Power characteristics of model propeller used in the powered-model tests.

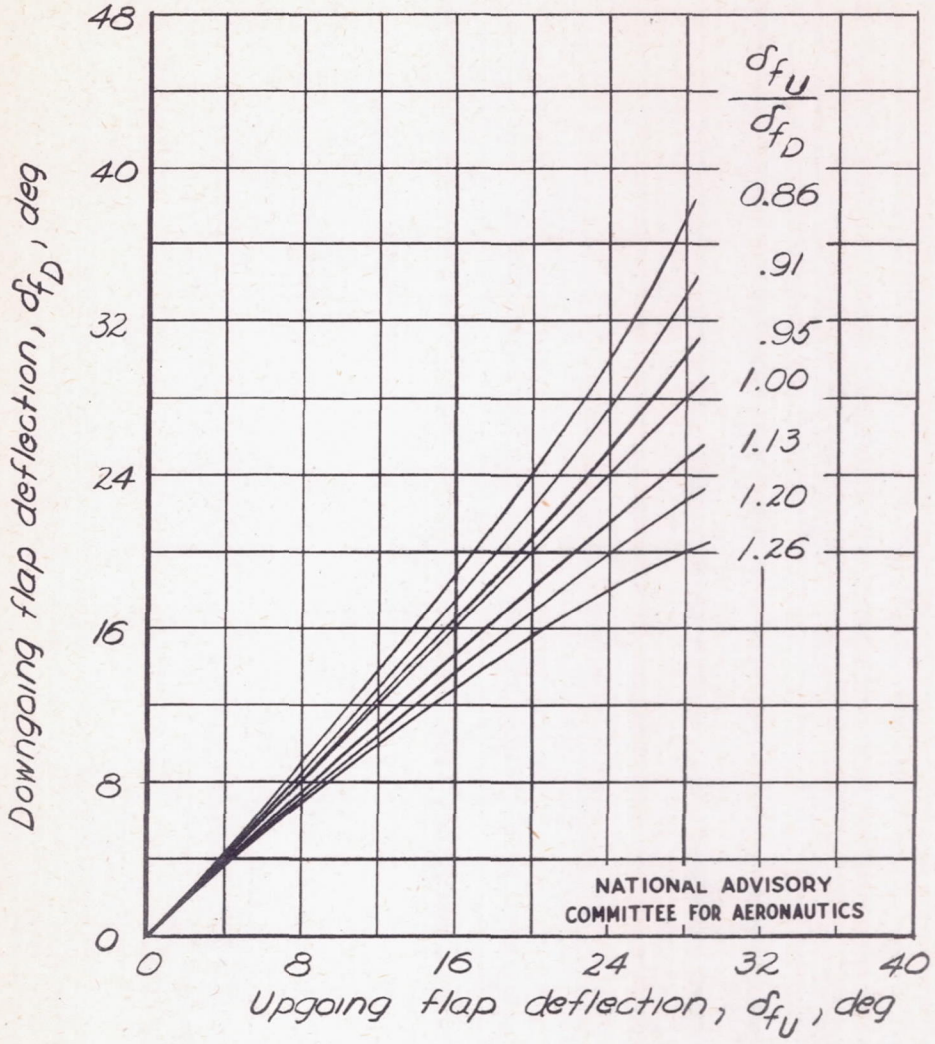

Figure 12.- Representative calibration curves used to determine flap-differential ratio on powered test model; 0° equals 40° initial deflection.

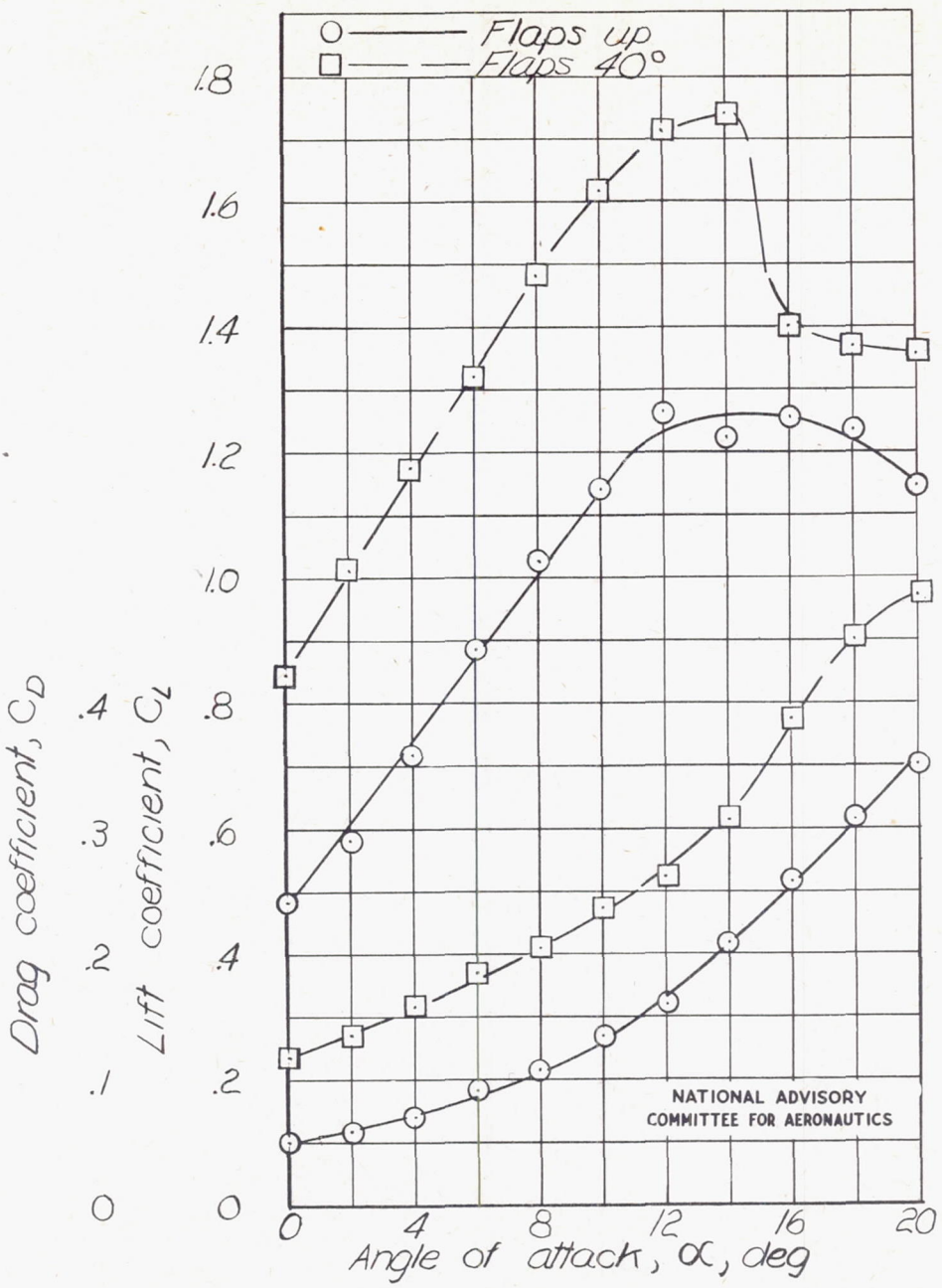

Figure 13.-Lift and drag characteristics of powered test model employed in tests of differential flap systems. Propeller-off condition; $\psi = 0°$; $q = 1.90$ pounds per square foot.

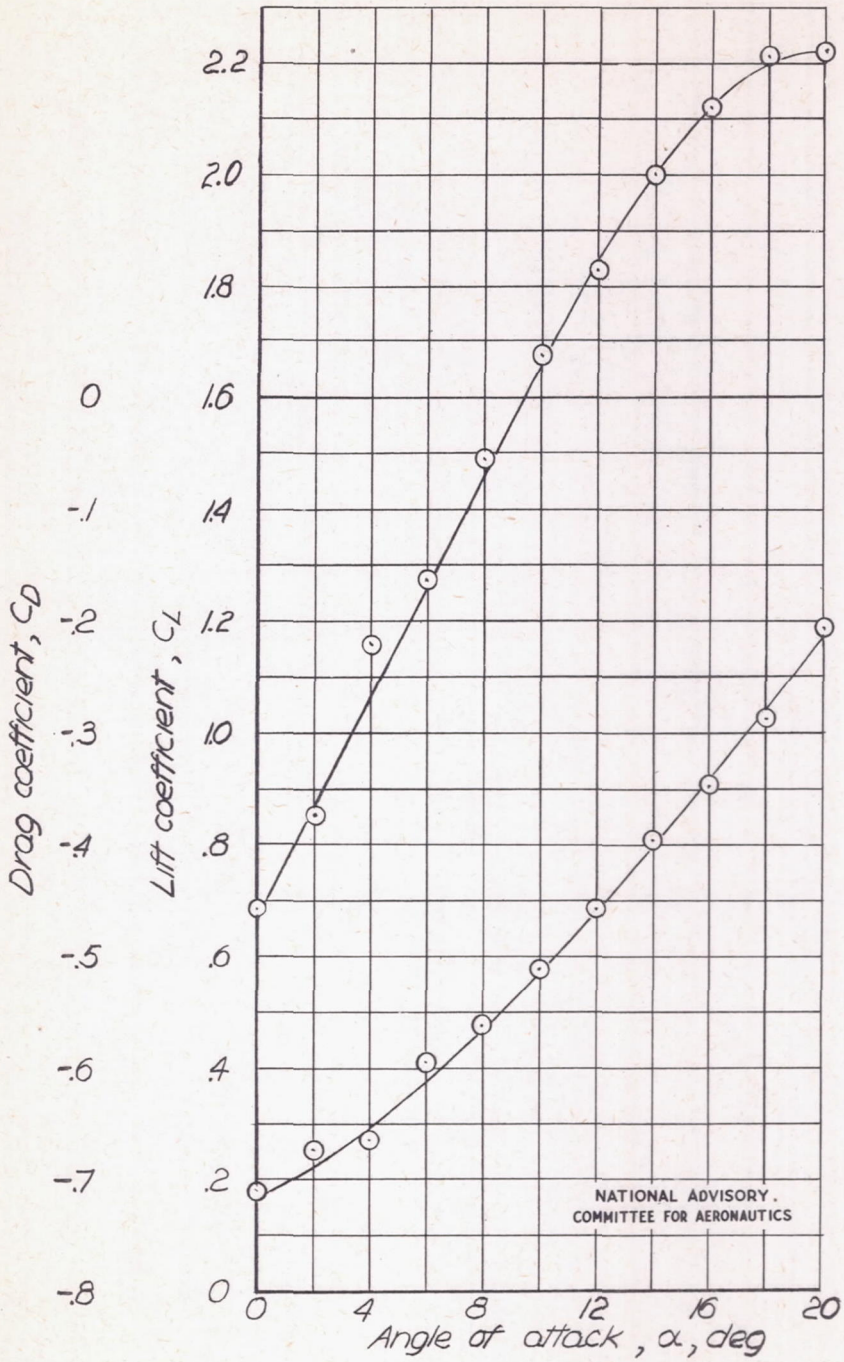

Figure 14.-Lift and drag characteristics of powered test model employed in tests of differential flap systems. $T_c = 0.96$; $\delta_f = 0°$; $\psi = 0°$; $q = 1.90$ pounds per square foot.

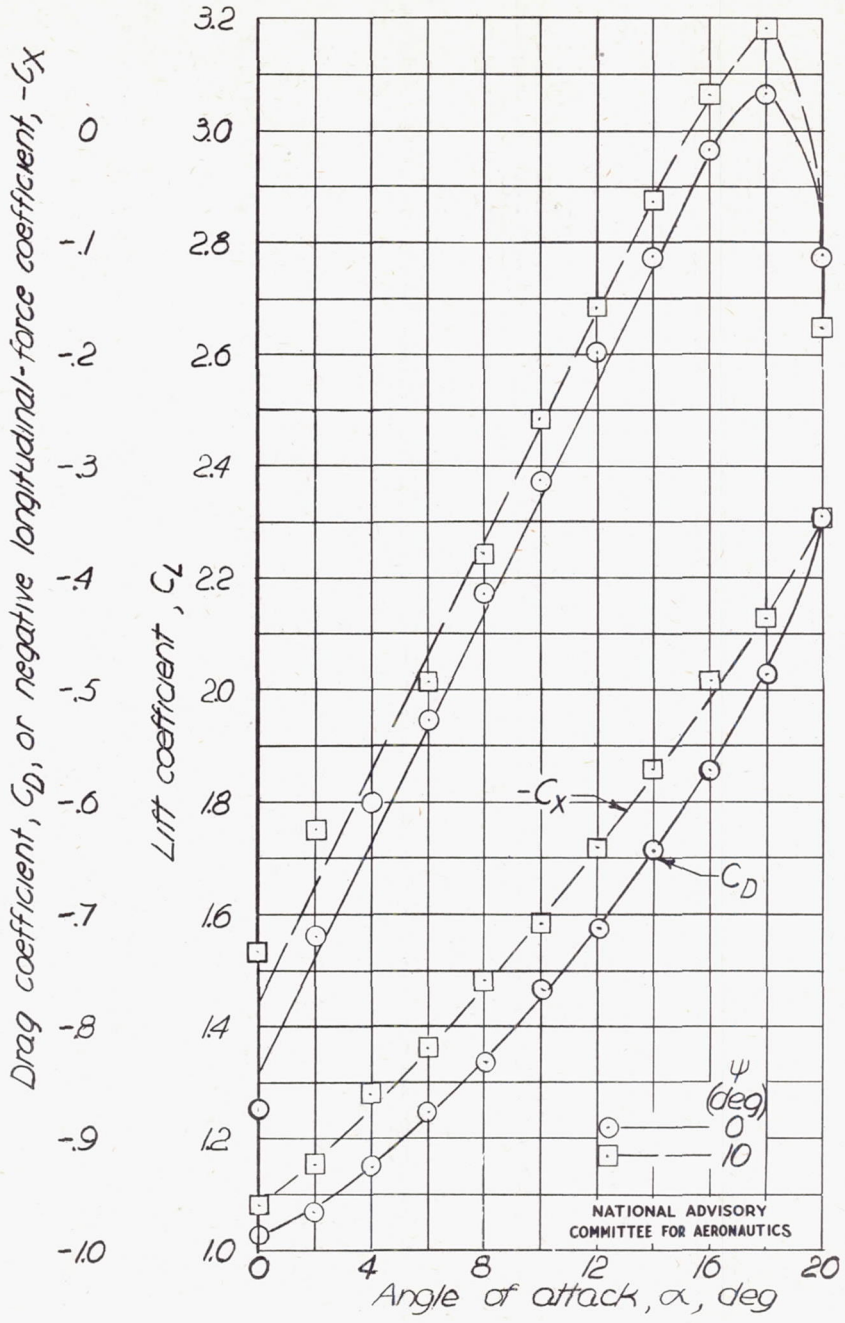

Figure 15.- Lift and drag characteristics of a powered test model employed in tests of differential flap systems for two angles of yaw. $T_c = 0.96$; $\delta_f = 40°$; $q = 1.90$ pounds per square foot.

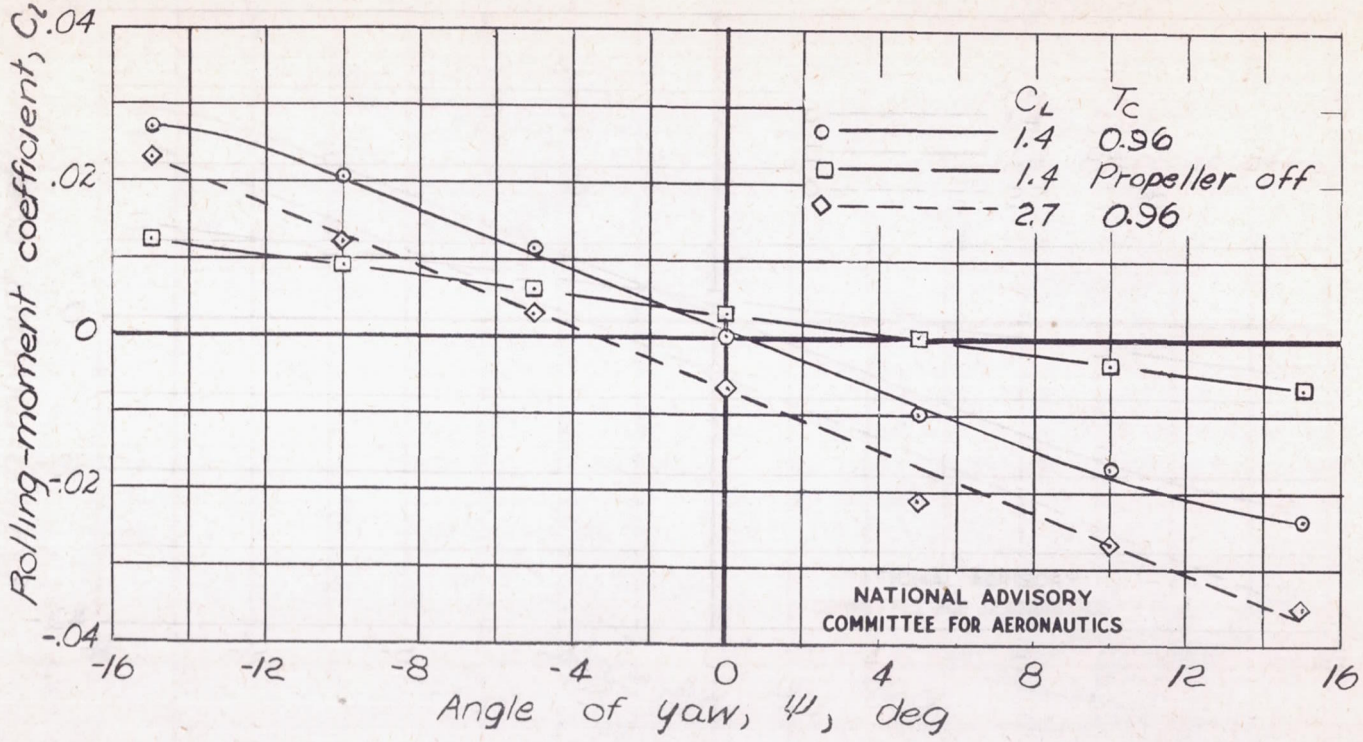

Figure 16.- Effect of power application and lift coefficient upon the dihedral characteristics of a low-midwing powered test model. Flaps locked at 40° ; q=1.90 pounds per square foot.

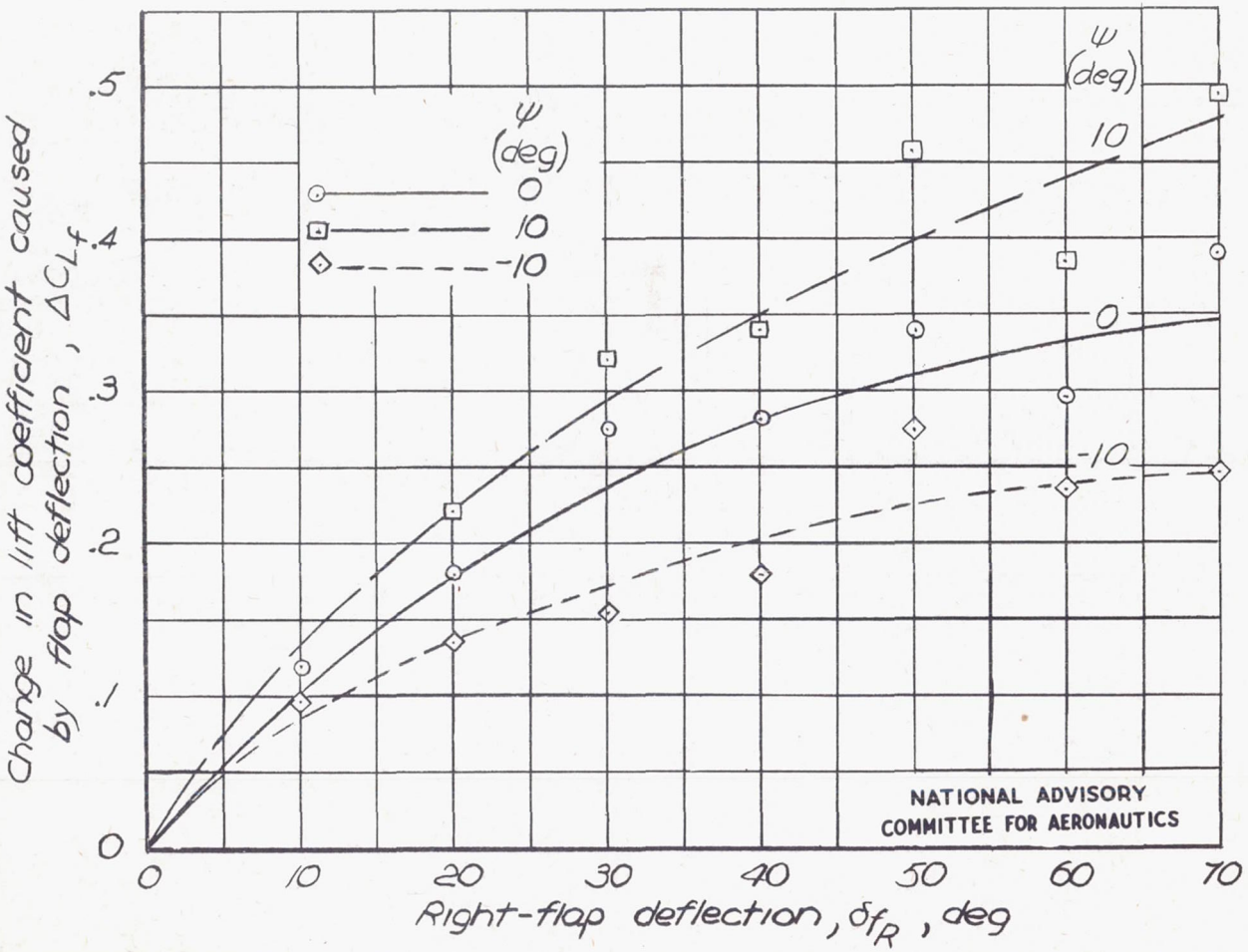

Figure 17.–Effectiveness curves of flap system employed on powered test model. $\alpha = 1.0°$; $T_c = 0.96$; $q = 1.90$ pounds per square foot.

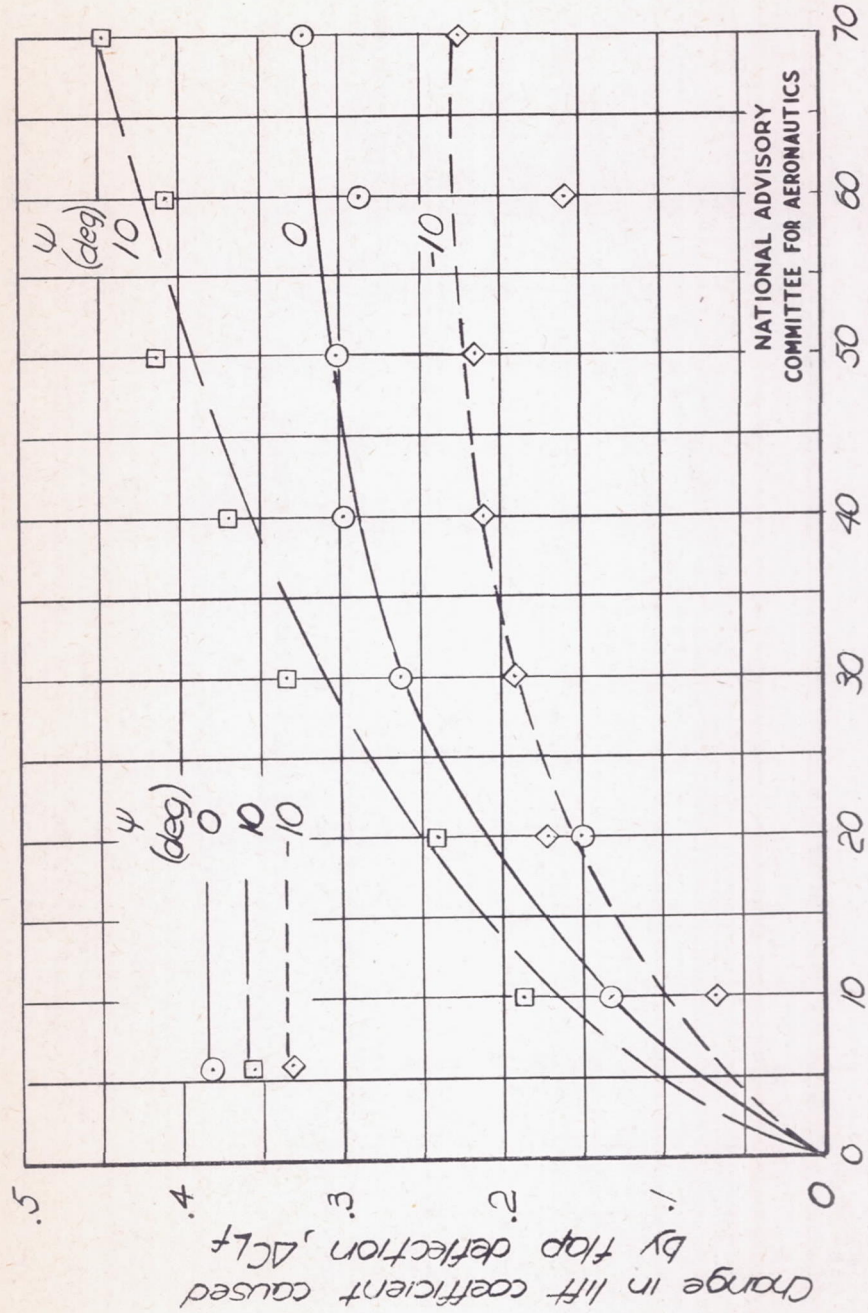

Figure 18.- Effectiveness curves of flap system employed on powered test model. $\alpha = 13.5^\circ$; $T_c = 0.96$; $q = 1.90$ pounds per square foot.

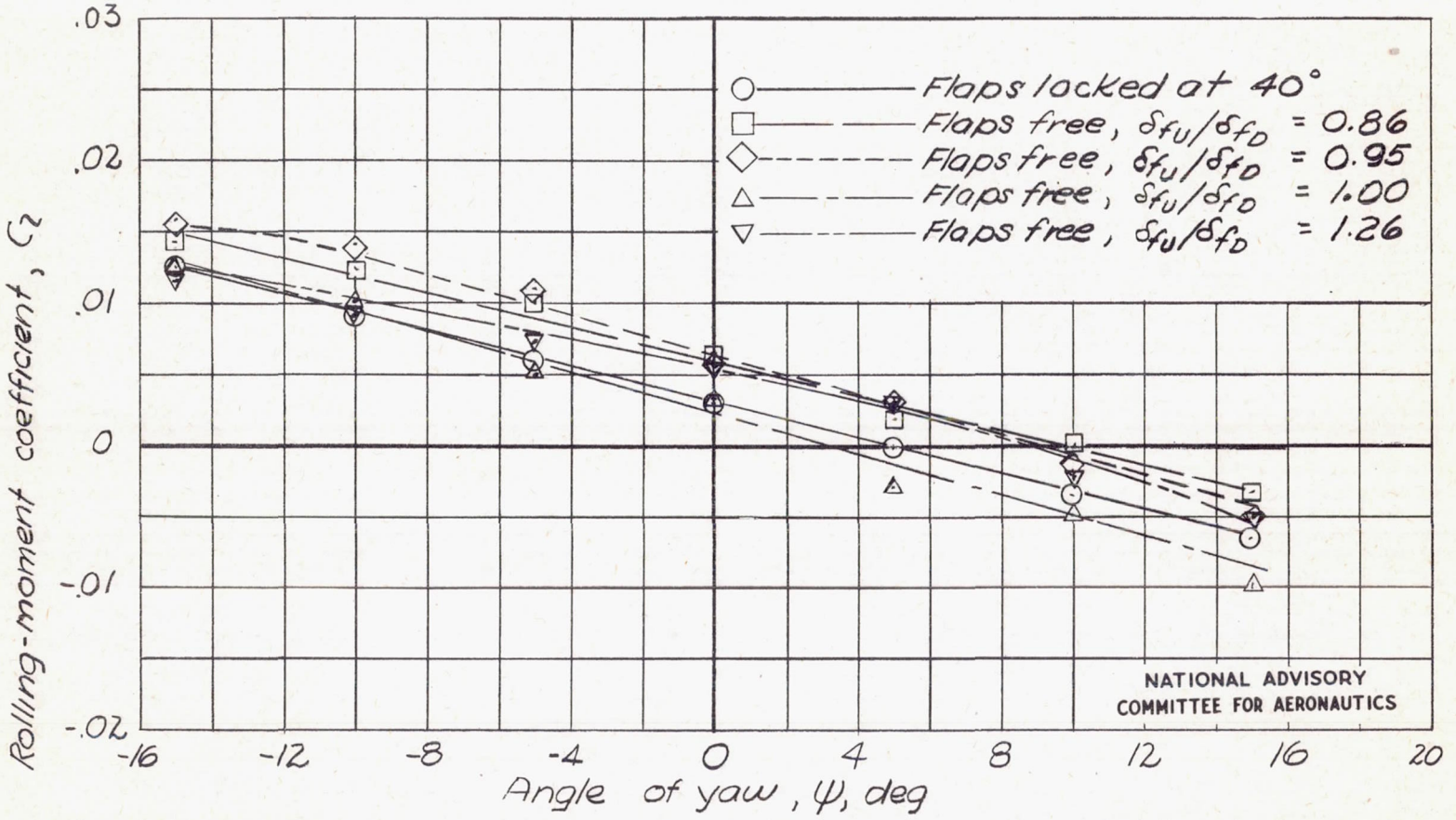

(a) Propeller off; $C_L = 1.4$.

Figure 19. - Effect of differential flap action upon the rolling-moment characteristics of test model in yaw. $q = 1.90$ pounds per square foot.

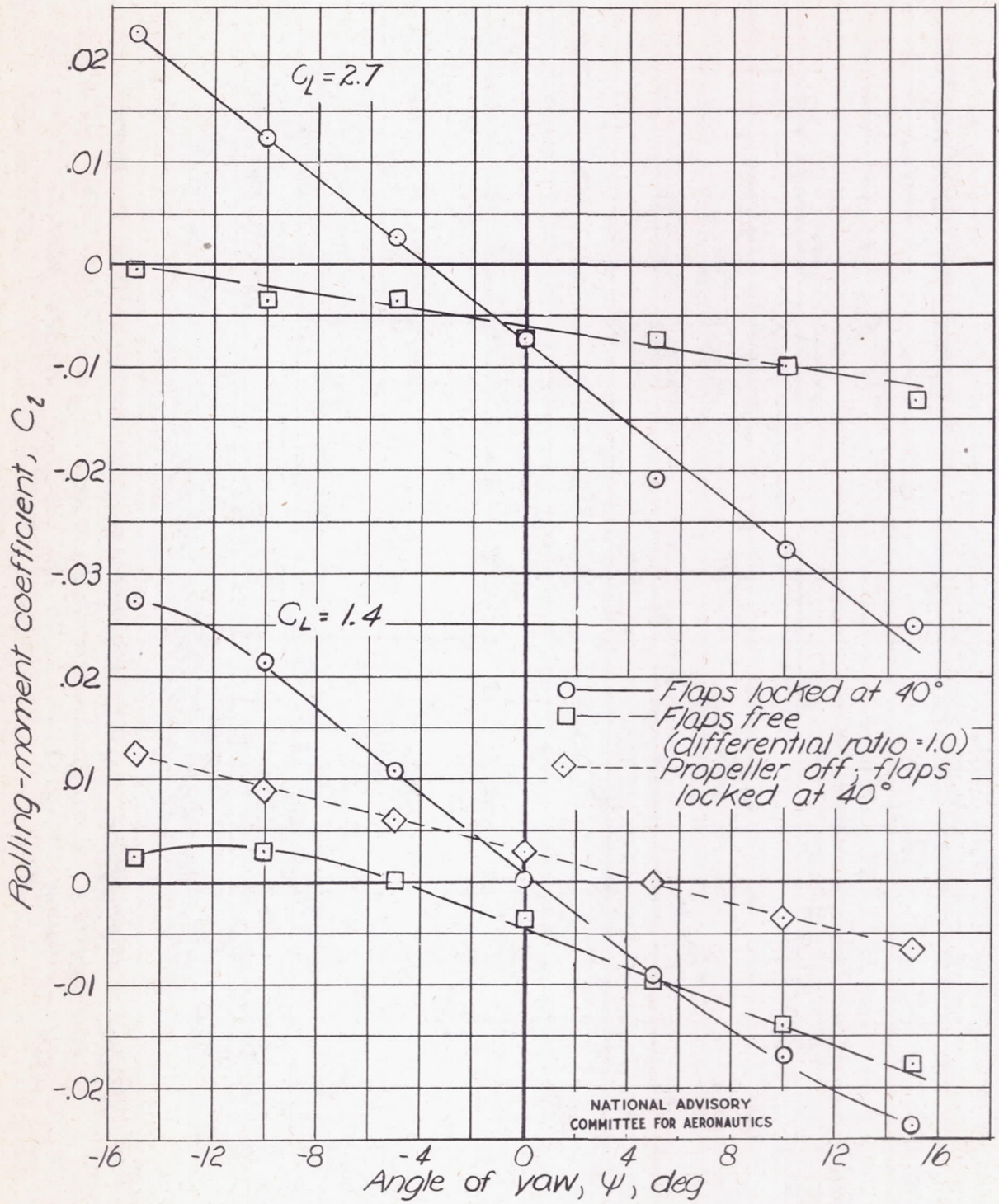

(b) $T_c = 0.96$ (unless otherwise indicated).

Figure 19.- Concluded.

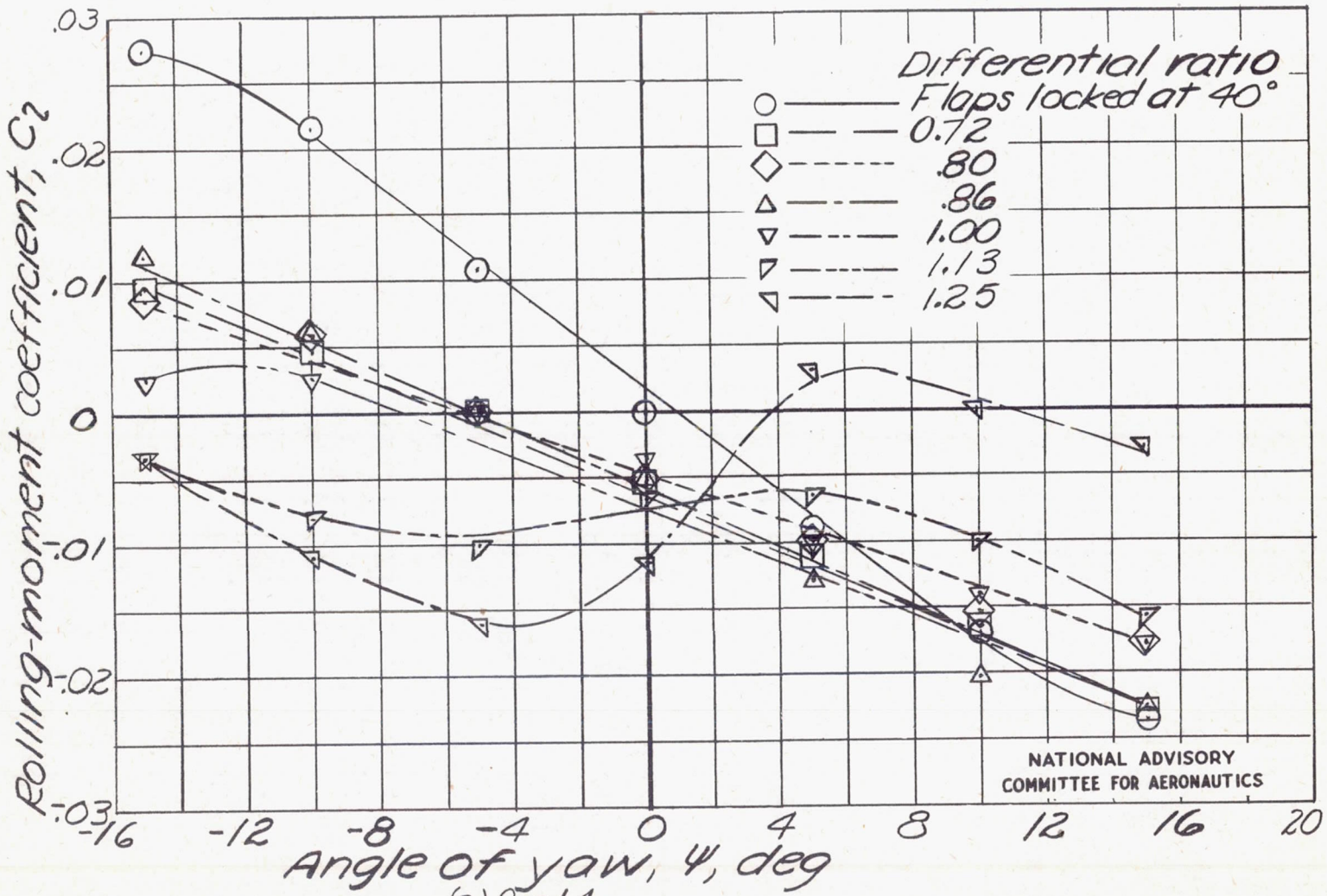

(a) $C_L = 1.4$.

Figure 20.- Effect of flap-differential ratio upon the rolling-moment characteristics of a powered test model in yaw. Flaps free except as noted; $T_C = 0.96$; $q = 1.90$ pounds per square foot.

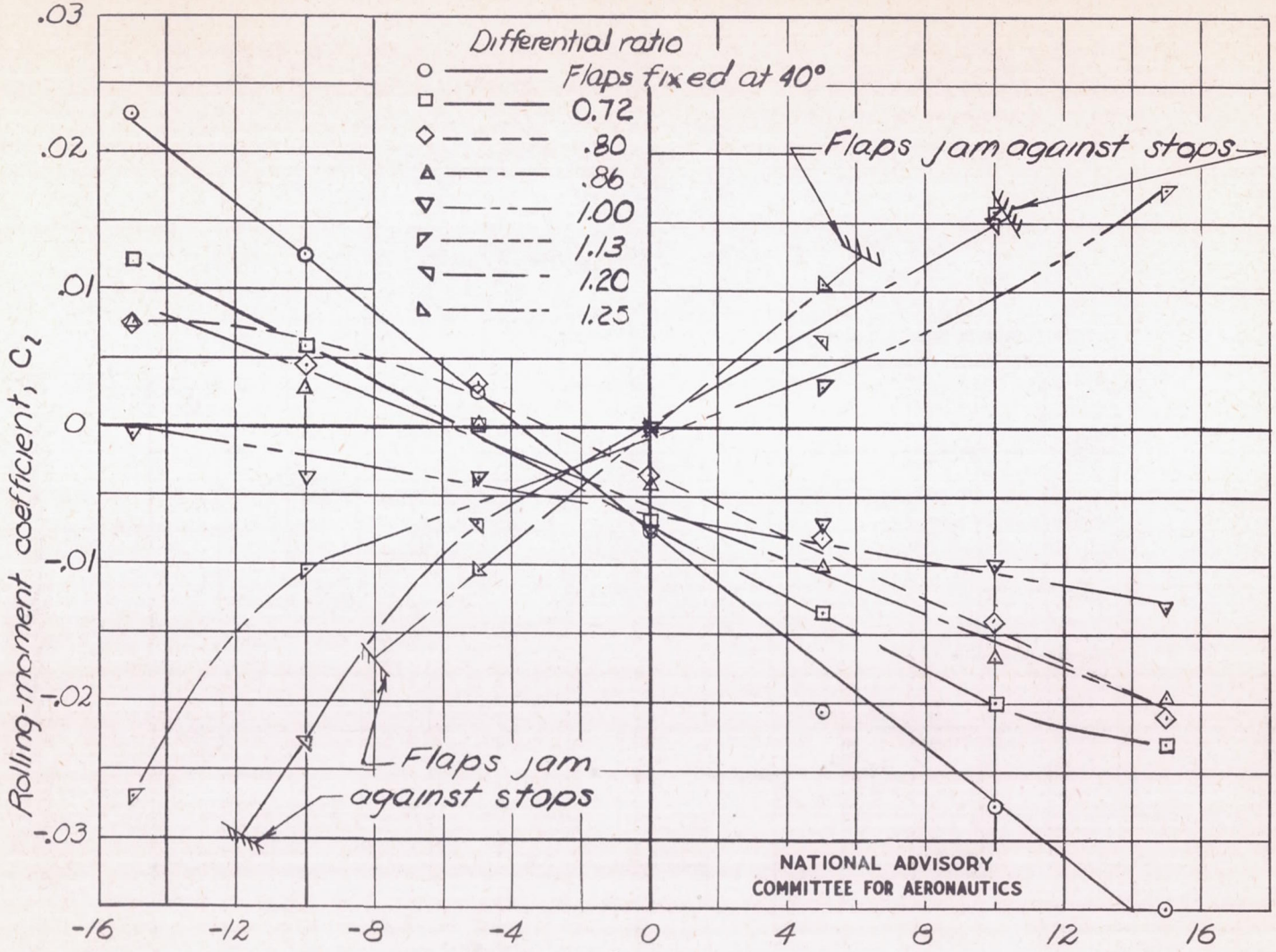

(b) $C_L = 2.7$.

Figure 20.- Concluded.

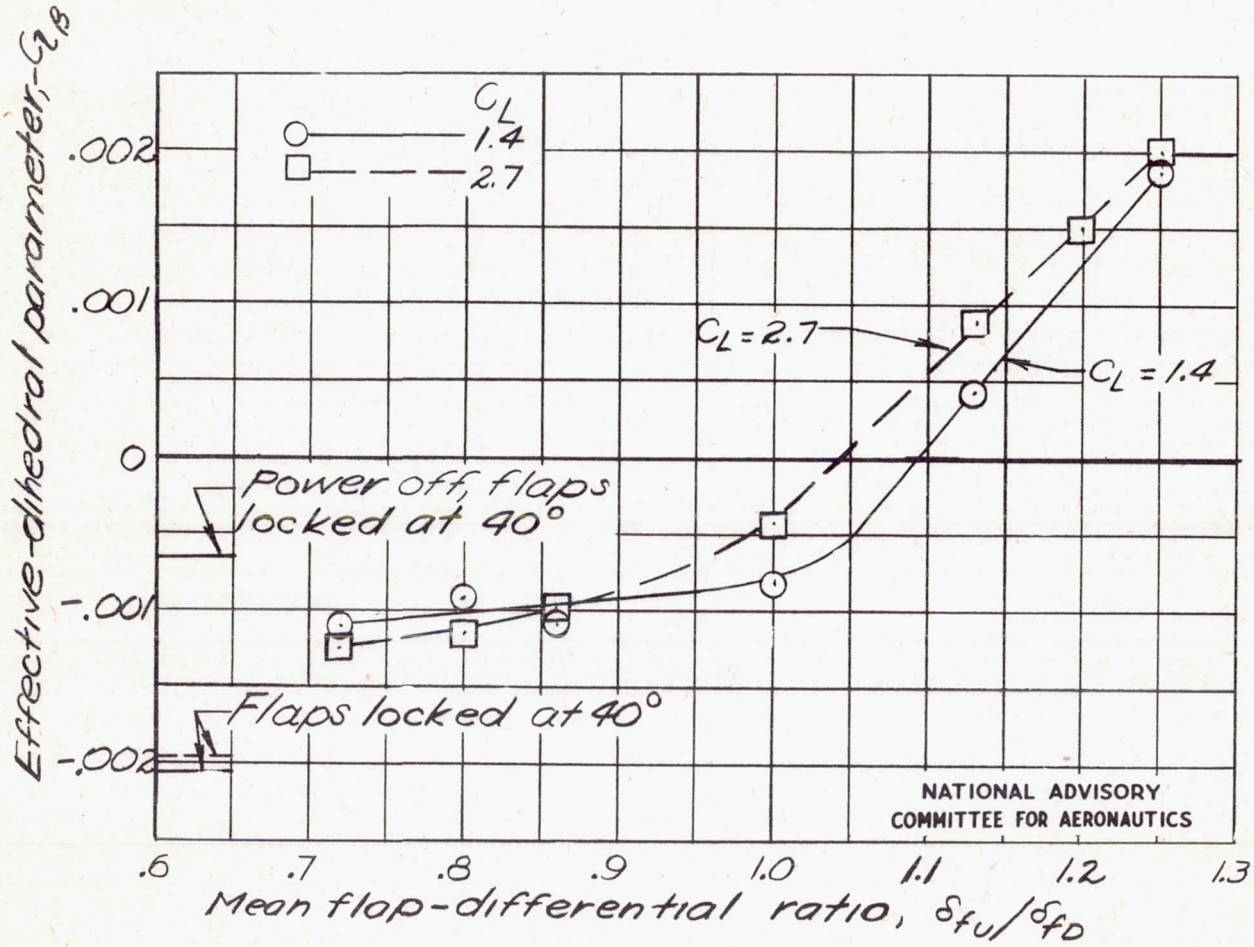

Figure 21.- Effect of flap-differential ratio upon the effective-dihedral characteristics of a powered test model. $T_c = 0.96$ (unless otherwise indicated); $q = 1.90$ pounds per square foot.

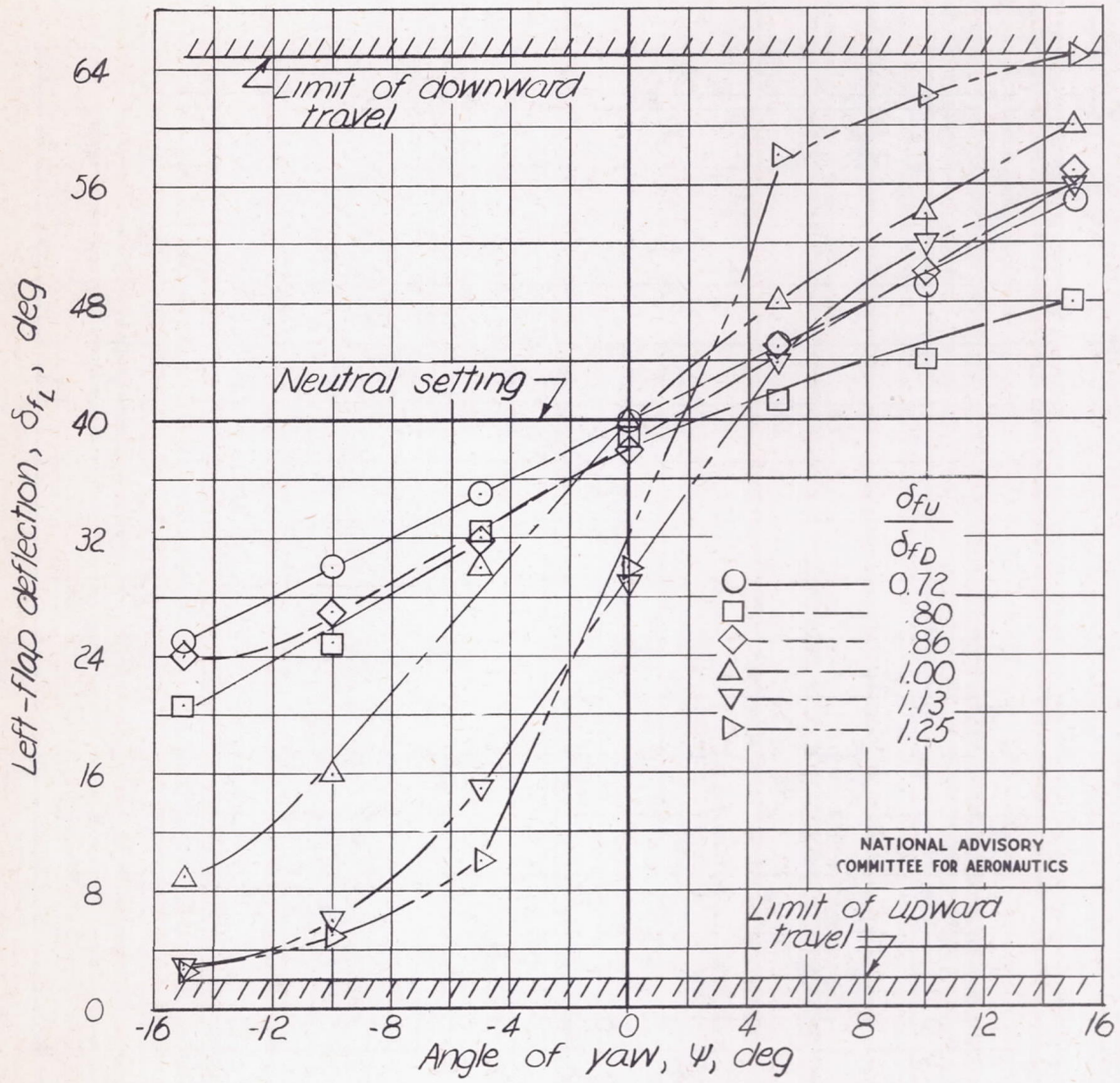

(a) $\alpha = 1.0°$; $C_L = 1.4$.

Figure 22.- Effect of flap-differential ratio upon the trim position of a free-floating differential flap system. Flaps jam against stops at all angles of yaw when $\delta_{fU}/\delta_{fD} > 1.4$. $\bar{T}_c = 0.96$; $q = 1.90$ pounds per square foot.

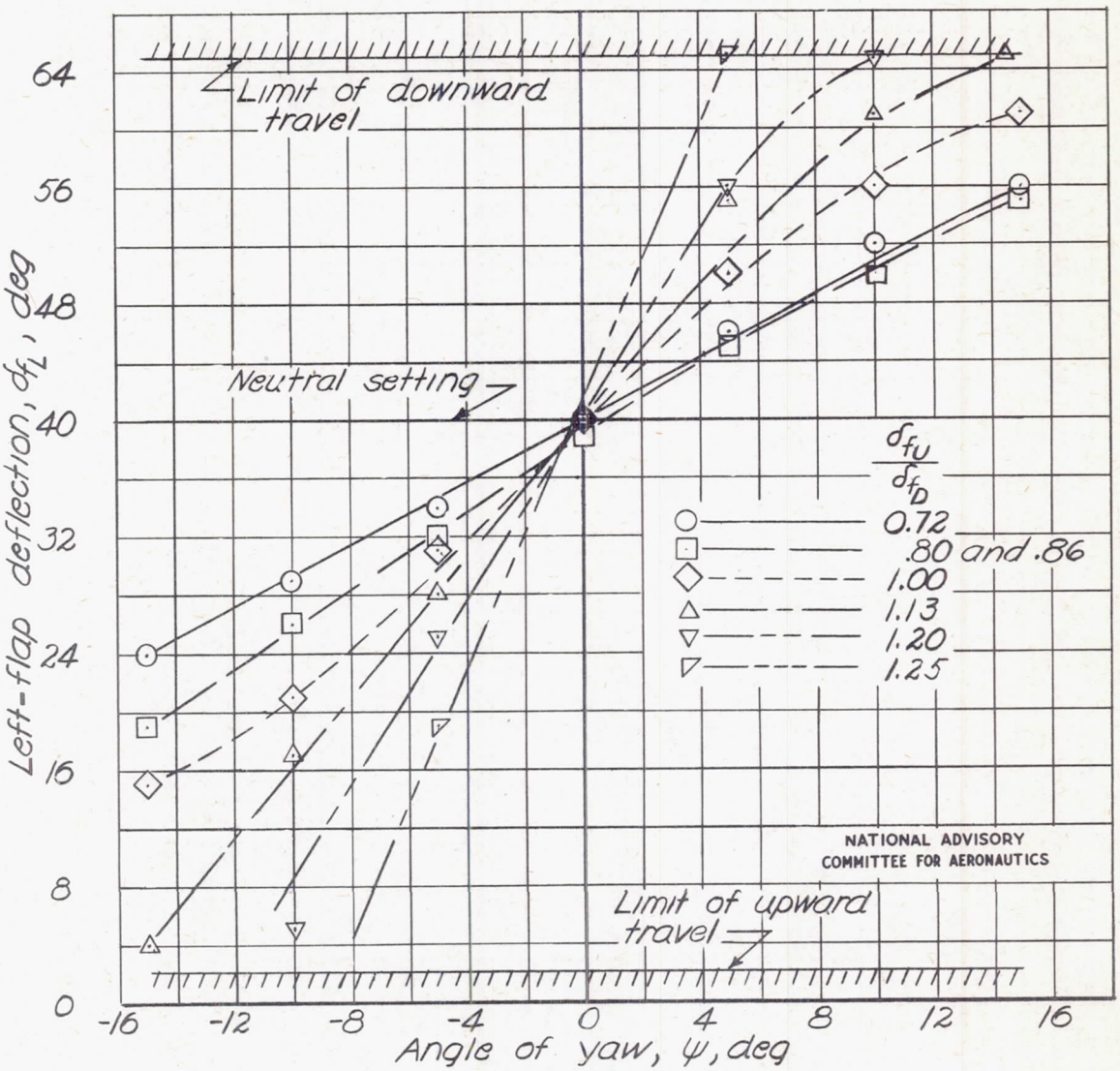

(b) $\alpha = 13.5°$; $C_L = 2.7$.

Figure 22 .- Concluded.

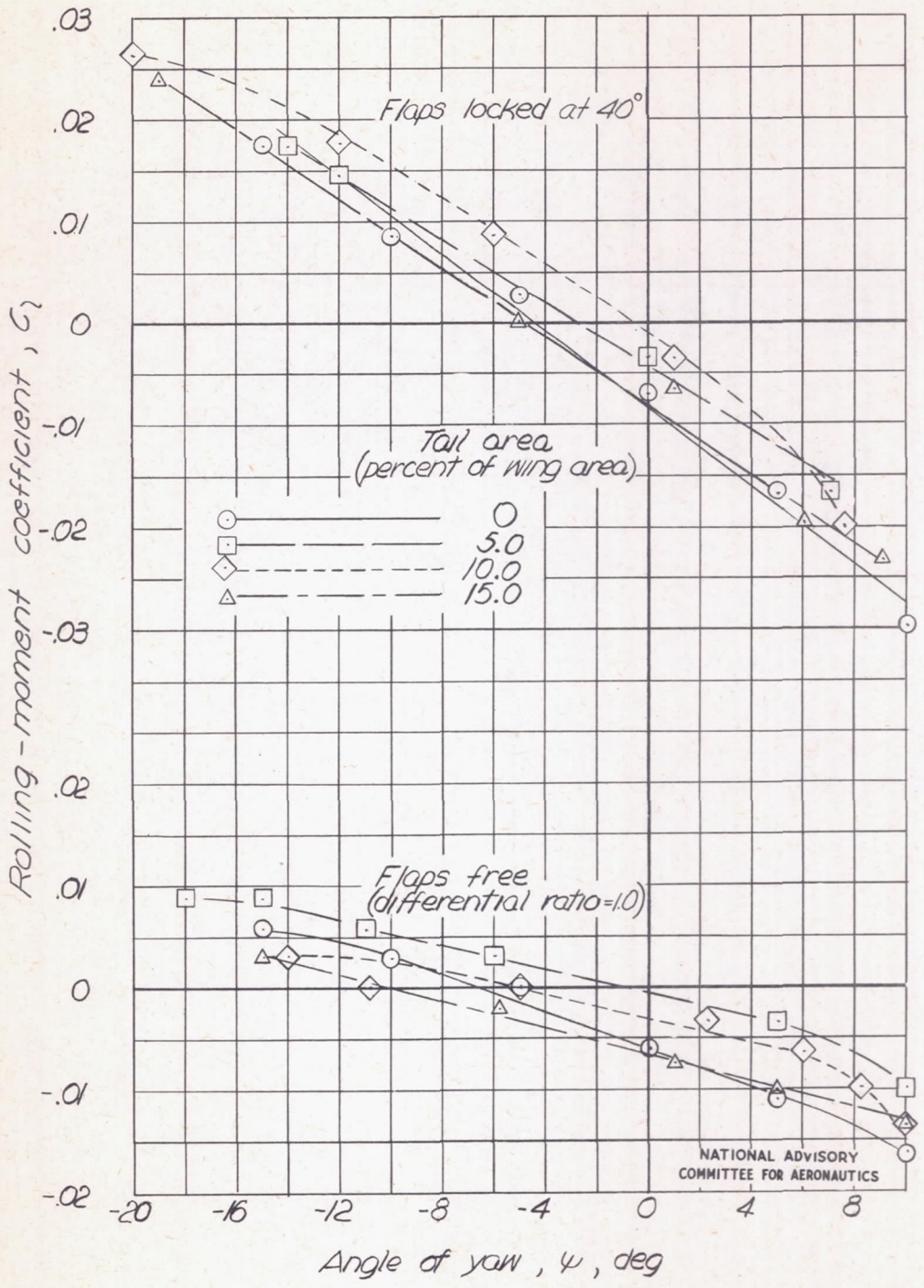

Figure 23.- Effect of vertical-tail area on the rolling-moment characteristics of a powered test model in yaw. $T_c = 0.96$; $C_L = 2.7$; $q = 1.90$ pounds per square foot.

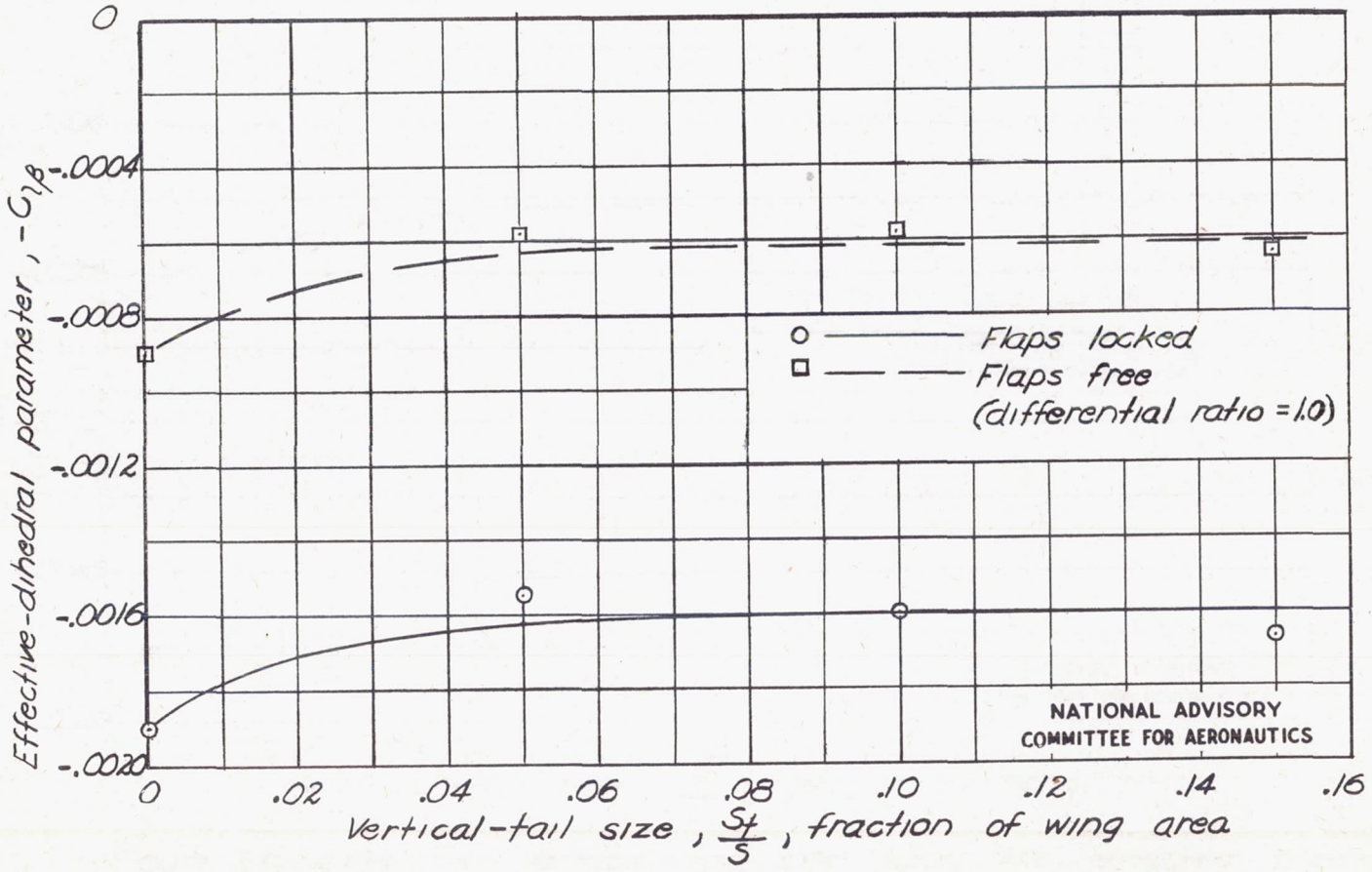

Figure 24.- Effect of vertical-tail area upon the effective-dihedral characteristics of a powered test model. $T_c = 0.96$; $C_L = 2.7$; $q = 1.90$ pounds per square foot.

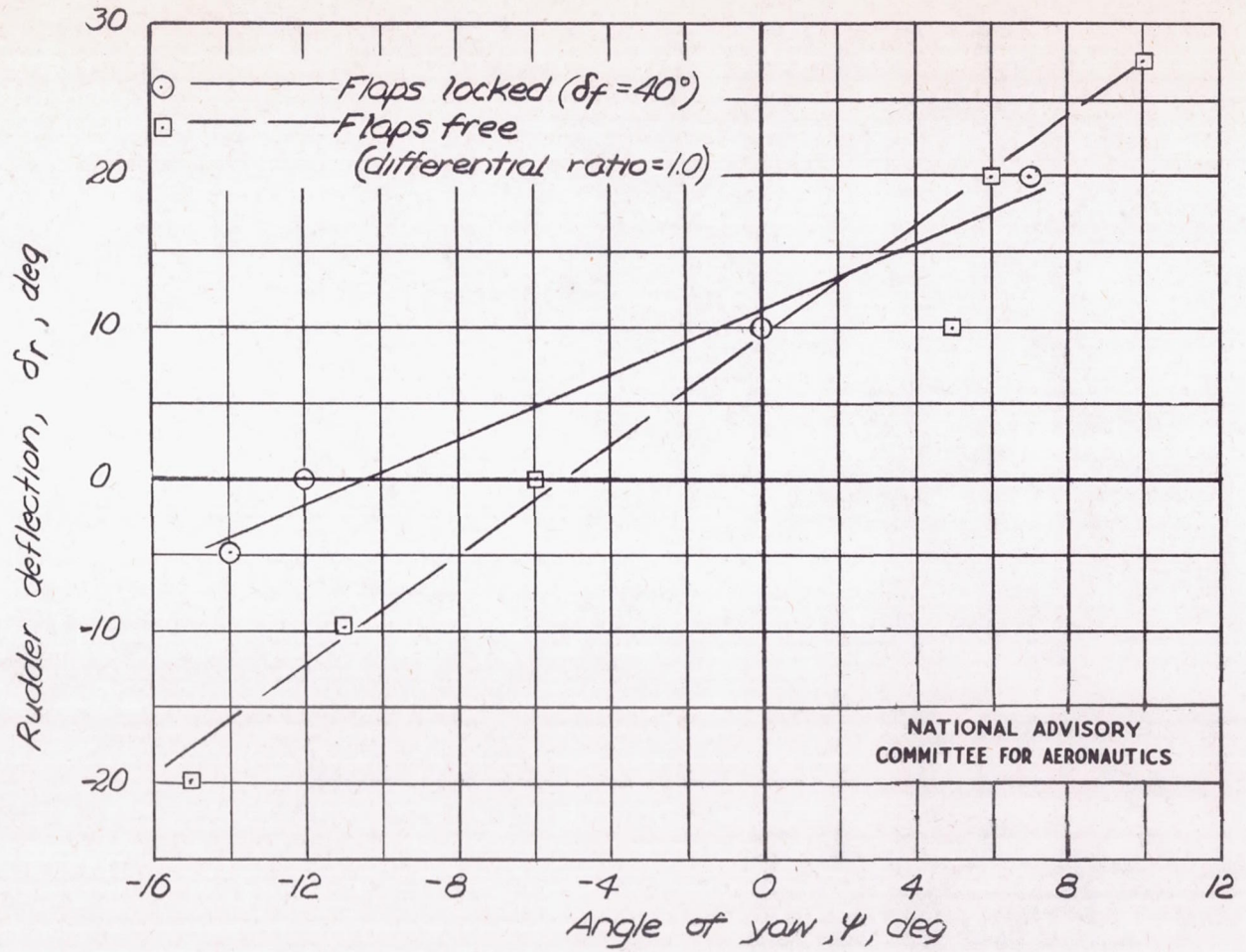

Figure 25.- Effect of freeing differential flaps upon the static directional stability. $T_c = 0.96$; $C_L = 2.7$; $S_t = 0.05S$; $q = 1.90$ pounds per square foot.